AeroChem Research Laboratories, Inc.
a subsidiary of PFAUDLER PERMUTIT, INC.
P. O. BOX 12, PRINCETON, N. J.
PHONE: WAlnut 1-7070

TP-60

Radiation Cooling of Aerodynamically Heated Surfaces at High Mach Numbers*

DANIEL E. ROSNER

ABSTRACT

In this paper several novel aspects of radiation cooling are discussed; particularly those associated with the occurrence of surface catalyzed atom recombination at high Mach numbers. An analogy between radiation cooling and chemical surface catalysis is explored and the dominant effects resulting from interactions between these two processes are illustrated using simple mathematical models which serve to single out the important nondimensional parameters. In connection with flight applications, altitude-velocity maps are presented which provide an overall picture of the regimes in which chemical nonequilibrium effects should be noticeable. Several unexplored areas of potential interest in the design of hypersonic lifting vehicles are outlined and related to the available literature. Interestingly enough, not all of these areas deal with thermochemical effects. Many "classical" problems remain unsolved, as illustrated by a brief discussion of the radiation cooled flat plate.

January 28, 1962; Paper to be presented at the AGARD Twenty-First Meeting of the Combustion and Propulsion Panel: Supersonic Flow, Chemical Processes and Radiative Transfer, London, England, April 1-5, 1963.

*This research was supported in part by the U. S. Air Force Office of Scientific Research, Propulsion Division, under Contract# AF 49(638)-1138

1. INTRODUCTION

The surface temperature at each point along an object traveling at high speed through a planetary atmosphere will seek a value at which the rate of heat input by convective processes* exactly balances that lost by phase change, radiation and internal heat conduction. Depending largely upon velocity and free stream density level, thermal radiation from the surface may be adequate to prevent appreciable phase change and, can, in fact become the dominant form of heat removal. It is therefore of interest to inquire: (i) what local surface temperatures would result?, and (ii) how would the surface temperatures vary with environmental conditions? To cite a particular example of current interest (1 - 3), it is known that local deceleration of the gaseous medium relative to a high speed entry object gives rise to temperature levels at which even the most stable molecules are fragmented, (e.g. nitrogen in the atmospheres of the earth and mars). This may occur either behind the bow shock wave that stands off blunt nosed bodies or in the shear layer near lateral surfaces as a result of locally intense viscous heating. When the gaseous medium experiences this kind of thermochemical change steady state surface temperatures may be expected to depart considerably from those corresponding to the aerodynamically equivalent motion through a chemically "inert" atmosphere (4).† Because of the dominant role which surface temperature plays in the determination of physical and chemical integrity,

---

*gas cap radiation to the surface will not be included in the present discussion. As will be seen, this radiation is usually negligible in the flight regimes in which cooling solely by radiation becomes feasible.

†an "inert" atmosphere can be visualized as one in which the kinetics of the thermochemical changes (e.g. dissociation, ionization) are not sufficiently fast for objects in the size range of interest.

particular emphasis must be placed on its accurate prediction using available physico-chemical information, experimental heat transfer data (usually obtained in the absence of complete simulation) and, of course, theory. However our purpose here is not so much to present accurate computational methods as it is to illustrate, by means of relatively simple examples, what dominant effects are likely to be encountered and in what flight domains. This admittedly limited goal is nowhere more evident than in our treatment of thermochemical effects, where it will be appreciated that the problem of making accurate predictions is computationally, if not conceptually, complex. While the radiation cooling of lifting re-entry vehicles, micrometeorites, and jet aircraft is implicit in much of the discussion which follows it should be mentioned that similar considerations would apply to the radiation cooling of nuclear rocket nozzles in outer space (5) or in more mundane applications, such as the determination of radiation errors in the pyrometry of flame gases (6), or the laboratory use of differential catalytic probes in the determination of local free-radical concentrations in nonequilibrium flow systems (7, 8).

Happily, many important aspects of radiation cooling are now well known, (9 - 13) and graphs have become available to facilitate the determination of steady state surface temperatures at various points along aerodynamic shapes of simple geometric form (11 - 13). However the design problem is by no means solved since available results are far from universally applicable. Indeed, technological advance continues to introduce new parameters at a rate which poses an intellectual challenge which must be met if this advance is to be sustained at reasonable cost.

For definiteness, consider the surface temperature predictions shown in Fig. 1, constructed from the recent work of Naysmith and Woodley (11). Here are collected the predicted steady state temperatures of slender surfaces whose emissivity is taken as 0.3 (being representative of polished metals). Results are applicable to streamwise location x = 1 ft. and cover the flight Mach number range 5 to 10 at two

altitudes. Three important features are immediately evident. First, surface temperatures are considerably below the corresponding gas dynamic recovery temperatures, particularly for high altitude flight. Thus, for Mach 10 flight at 200 Kft, the local surface temperature is estimated to be only 840°K whereas the gas-dynamic recovery temperature in the absence of dissociation would be about 6060°K at this same flight condition. If one were limited by a sudden loss of strength or, say, by local melting, neglect of radiation would therefore provide a very pessimistic estimate of the maximum attainable Mach number based on aerodynamic heating considerations alone. Second, in the absence of internal heat conduction considerable surface temperature nonuniformity would exist, as evidenced by the fact that the local temperature is always much lower than the (mean) temperature which would have existed had the total heat imput from the leading edge to the point in question been distributed uniformly over that distance. For the case cited above this temperature difference amounts to some 160°K. The very existence of large streamwise temperature variations, especially for laminar boundary layers, raises the question of the validity of using isothermal surface heat transfer coefficients (9). This question will be discussed in Section 2.2. Finally, surface temperatures are very sensitive to the fluid dynamic state of the boundary layer and are much larger if the boundary layers are turbulent, reflecting the enhanced conditions of heat input. At $M_\infty = 10$, h = 50 Kft., for example, a turbulent boundary layer would cause local surface temperatures to be some 490°K larger than in the case of laminar boundary layers, bringing the steady state surface temperatures to above 2000°K.

While the error in these results was estimated by the authors to be only about 10 percent, at intermediate altitudes and high Mach numbers the kinetics of oxygen dissociation and recombination could begin to influence results of this type considerably, as would be suggested, for example, by the difference between the real and

ideal stagnation temperatures computed at the free stream pressure.* In fact, it will be shown that the steady state surface temperature can be either higher or lower than that estimated on the basis of ideal gas calculations (10). Moreover, owing to the possibility of exothermic atom recombination within the boundary layer or at the radiating surface itself the surface temperature at a nose cap or leading edge can certainly be much greater than the real gas stagnation temperature. Thus, much of the data contained in available design charts should be interpreted in the light of the chemical kinetic considerations (cf. Part 3). Finally, in realistic situations chemical kinetics can introduce entirely new phenomena [e.g. surface temperature hysteresis (14)] as well as modify the "expected" dependence of surface temperature on, say, physical scale (15). New design parameters (e.g. recombination coefficients) are thereby introduced into the materials selection problem, and, as such, this class of phenomena merits further attention.

2. RADIATION COOLING IN THE ABSENCE OF CHEMICAL REACTION

In a remarkable paper on the theory of laminar boundary layers, Lighthill (9) pointed out that since the wall temperature distribution $T_w(x)$ of a radiation cooled body is itself non-uniform, a theory strictly applicable under this nonisothermal condition is required to compute it. Using a method which is in fact asymptotically exact in the limit of infinite Prandtl number† he was able to show that the true steady state temperature distribution $T_w(x)$ is obtainable from the solution of a nonlinear, singular Volterra integral equation. For a flat plate of zero thermal conductivity and constant emissivity, slowly convergant expansions for the steady state temperature

---

*for slender objects; for blunted shapes this difference is reduced owing to the higher pressure levels encountered.

†While Lighthill discussed applications to laminar flow only in the limit $Pr_\lambda \to \infty$ his basic solution is applicable to turbulent flow as well, since the thermal boundary is then fully immersed in the laminar sublayer (16).

distribution were obtained (for small x and large x) containing fractional powers of the streamwise coordinate x. Lighthill did not investigate the overall radiative transfer from such plates, or the validy of approximate methods which make local use of "isothermal" heat transfer coefficients, $Nu_{iso}(x)$. Yet it is clear from Lighthill's series solution that near the leading edge of the plate Nu/Nu_{iso} approaches the finite value 1.3689, with Nu/Nu_{iso} approaching unity only far downstream (as $x \to \infty$). In 1958 N. Curle (17) applied an approximate method for calculating the surface temperature distribution of a radiation cooled flat plate. While his approximation reduces the problem to an algebraic (4th degree) equation, it is readily shown to be far less accurate than straightforward application of $Nu_{iso}(x)$ to the same problem; a technique which also leads directly to an algebraic equation of identical form. In the light of this background the remainder of this section will therefore be devoted to (i) a brief examination of the accuracy of the $Nu_{iso}(x)$ approximation for both laminar and turbulent boundary layer (ii) the development of an improved approximate method readily applicable to laminar or turbulent boundary layer flow over surfaces with temperature dependent emissivity, and (iii) a comparison between the overall radiative transfer from plates of zero and infinite thermal conductivity (10). It will be shown that the radiation cooling problem is, mathematically, strictly analogous to a problem in the diffusional theory of surface catalyzed chemical reactions (10, 18, 19). This analogy will, in fact, provide a natural link with the remainder of this paper, devoted in part to the effect of exothermic surface reactions in radiation cooling situations.

2.1 A Further Analogy in Transport Theory (10)

Following Lighthill (9), let us begin our discussion of radiation cooling at high Mach numbers with a treatment of the incompressible, $M_\infty \to 0$, planar problem!

In that case the radiation-cooling chemical surface catalysis analogy is readily demonstrated as follows. Consider the flow configurations depicted in panels 1 and 2 of Fig. 2. Panel 1 shows the incompressible flow of a hot, nonabsorbing fluid over a convex cylinder of zero thermal conductivity.* In the steady state each element of surface will radiate heat away at exactly the rate reaching it by convection from the main stream, i.e.

$$\lambda \cdot \left(\partial T / \partial y \right)_{y=0} = \epsilon_w \cdot \sigma \left(T^4 \right)_{y=0} \tag{1}$$

Here λ is the thermal conductivity of the fluid, ϵ_w is the total hemispheric emissivity of the surface, σ is the Stefan-Boltzmann radiation constant, and T represents the local fluid temperature (assumed equal to the solid surface temperature at y = 0). In general, ϵ_w is itself temperature dependent so that the product $\epsilon_w \sigma T_w^4$ may be taken to vary as, say, the nth power of local surface temperature, where

$$n \equiv 4 + d \ln \epsilon_w / d \ln T_w \tag{2}$$

For simplicity, it will be assumed herafter that n may be taken to be constant over the surface temperature range of interest, although different from 4. Some typical values of n are collected in Table 1, where it is seen that values between 2 and 6 are conceivably of practical interest, with most ceramic materials exhibiting $n < 4$ and metals exhibiting $n > 4$.

---

*In practice, this condition may be replaced by the condition of sufficiently thin walls or the use of segmented walls to prevent heat conduction in the streamwise direction.

At sufficiently large Reynolds numbers the velocity field in the neighborhood of the cylinder will satisfy the constant property boundary layer equation*

$$u\frac{\partial u}{\partial x} + v\frac{\partial u}{\partial y} = u_e\frac{du_e}{dx} + \frac{\partial}{\partial y}\left[(\nu + \epsilon_\nu)\frac{\partial u}{\partial y}\right] \tag{3}$$

where ν and ϵ_ν are, respectively, the kinematic viscosity and eddy viscosity of the fluid and $u_e(x)$ is the main stream velocity distribution around the cylinder. Similarly, at sufficiently large Peclet numbers, the temperature field $T(x,y)$ within the fluid will satisfy the constant property boundary layer equation

$$u\frac{\partial T}{\partial x} + v\frac{\partial T}{\partial y} = \frac{\partial}{\partial y}\left[\left(\frac{\nu}{Pr_\lambda} + \frac{\epsilon_\nu}{Pr_\lambda^{(\epsilon)}}\right)\frac{\partial T}{\partial y}\right] \tag{4}$$

where Pr_λ and $Pr_\lambda^{(t)}$ represent the laminar and turbulent Prandtl numbers for heat conduction. Now consider panel 2 of Fig. 2. Depicted here is the steady flow of an incompressible carrier fluid over an impermeable catalytic cylinder. Contained in the carrier fluid is a reactant (present in dilute amounts) which diffuses to the solid surface and reacts there at a rate which is some function of the local reactant concentration (mass fraction) α_w itself. Very frequently this phenomenological reaction rate law is well represented by a simple power law,† so that the reactant concentration field at the fluid/solid interface must satisfy the boundary condition

$$D\rho\cdot(\partial\alpha/\partial y)_{y=0} = k_w\left[(\rho\alpha)^n\right]_w \tag{5}$$

---

*The validity of the analogy described here is not contingent upon the validity of boundary layer theory; however, the analogy will be illustrated later for the case of boundary layer flow over a flat plate.

†an important example for which this is not true is given in Section 3.3 (23)

where k_w is called the intrinsic catalytic activity of the surface, n is the true reaction order and D is the Fick diffusivity for reactant diffusion through the carrier fluid. For a single material at uniform surface temperature the two parameters k_w and n then completely define the chemical kinetic characteristics of the surface.

The velocity field in the neighborhood of the catalyst will be identical to that in panel 1 and, moreover, in the absence of chemical reaction in the fluid phase the concentration field will satisfy the constant property boundary layer equation

$$u\frac{\partial \alpha}{\partial x} + v\frac{\partial \alpha}{\partial y} = \frac{\partial}{\partial y}\left[\left(\frac{\nu}{Pr_D} + \frac{\epsilon_\nu}{Pr_D(t)}\right)\frac{\partial \alpha}{\partial y}\right] \tag{6}$$

Far from the catalyst ($y \to \infty$) we have $\alpha(x,y) \to \alpha_e \equiv$ const. The mathematical similarity between the two problems is then evident since $T(x,y)$ and $\alpha(x,y)$ satisfy differential equations and boundary conditions of identical form. In particular, $T_w(x) \equiv T(x,o)$ and $\alpha_w(x) \equiv \alpha(x,o)$ are not known a priori but in fact constitute an important part of the solution. Thus, having obtained $T_w(x)$, one can calculate the local and overall rates of heat transfer (per unit depth) from the relations

$$\dot{q}''(x) = \epsilon_w \cdot \sigma \cdot \left[T_w(x)\right]^4 \tag{7}$$

$$Q = \int_o^L \epsilon_w(T_w) \cdot \sigma \cdot \left[T_w(x)\right]^4 dx \tag{8}$$

(for one side of a symmetrical cylinder). Similarly, having obtained $\alpha_w(x)$, one can obtain the local and overall rates of reaction (per unit depth) viz.

$$\dot{\mathcal{R}}''(x) = k_w \cdot [\rho \alpha_w(x)]^n \tag{9}$$

and

$$\dot{\bar{\mathcal{R}}} = \int_0^L k_w \cdot [\rho \alpha_w(x)]^n \, dx \tag{10}$$

(for one side of a symmetrical cylinder). The exponent n defined by Eq. (2) plays the same role in the radiation cooling problem as the true reaction order n in the diffusion surface catalysis problem. Interestingly enough, while the range 2 to 6 was seen to be of interest for radiating surfaces (cf. Table 1) in heterogeneous chemical kinetics one usually encounters values of the true reaction order n between 0 and 2. Thus, solutions covering the range $0 < n < 6$ would be of general interest in transport theory. When expressed in terms of nondimensional transfer rates and coordinates, the solution for $n = 2$ would then be directly applicable to either problem. The nature of the important nondimensional variables will be evident in discussing a particular case, viz. the radiation cooled flat plate.

2.2 Approximate Solution for the Radiation Cooled Flat Plate; Incompressible Case (10)

An approximate method which has already proven convenient for solving the diffusion-surface reaction problem will be outlined here and then used as the basis for a brief discussion of accuracy.

Ambrok (24) has provided a simple expression for estimating the effect of surface temperature variations $T_w(x)$ [or, more generally, $\vartheta_e(x) \equiv T_e - T_w$] on the local heat transfer coefficient. For a flat plate (cf. Fig. 3) his result can be cast in the Stanton number form

$$St(x) = St_{iso}(L)\left\{\left[\vartheta_e(x)\right]^{-\frac{\omega}{\omega-1}}\int_0^{x/L}\left[\vartheta_e(x)\right]^{\frac{\omega}{\omega-1}} d(x/L)\right\}^{-1/\omega} \quad (11)$$

where the exponent ω takes on the value 2 for laminar boundary layer flow, and 5 for turbulent boundary layer flow (tripped at leading edge). $St_{iso}(L)$ represents the appropriate value of the Stanton number at the trailing edge ($x = L$) in the event $\vartheta_e = \text{const}$. The success of this method can be conveniently tested against exact (similar) solutions for the case $\vartheta_e(x) \propto x^{\lambda}$, where λ is constant. Results over the λ-range of interest here ($0 < \lambda < \frac{1}{2}$) are shown in Fig. 4. Evidently, the method is quite satisfactory for both turbulent and laminar boundary layer flow provided the Prandtl number is not too small.* This being the case, consider the application of Eq. (11) to the radiation cooling problem. Using the definition of St(x) the boundary condition (1) takes the form

$$\epsilon_w \cdot \sigma\, T_w^4 = St(x) \cdot \rho\, u_e \cdot (T_e - T_w) \cdot c_p \quad (12)$$

where St(x) is given by Eq. (11) with $\omega = 2$ or 5. This nonlinear integral equation can, however, be converted to a separable ordinary differential equation and, thus, readily solved. At this point it is convenient to introduce the following nondimensional variables

*In the laminar case it is well known that the $Pr \to \infty$ asymptote provides an accurate estimate of transfer coefficients even for Prandtl numbers of order unity (25).

$$\theta \equiv T_w / T_e \tag{13}$$

$$\mathcal{R} \equiv \frac{\epsilon_w(T_e) \cdot \sigma T_e^4}{Nu_{iso}(L) \cdot \lambda T_e / L} \tag{14}$$

$$z \equiv \mathcal{R} \cdot (x/L)^{1/\omega} \tag{15}$$

Note that x is a stretched streamwise coordinate proportional to the local boundary layer thickness $\delta_{iso}(x)$. In terms of these variables Eq. (12) becomes

$$\theta^n \equiv (1-\theta)\left\{(1-\theta)^{-\frac{\omega}{\omega-1}} \int_0^z (1-\theta)^{\frac{\omega}{\omega-1}} \omega \xi^{\omega-1} d\xi\right\}^{-1/\omega} \tag{16}$$

which, upon differentiation, leads to a separable differential equation. This equation can then be integrated term-by-term as follows

$$\frac{z^\omega}{\omega} = \int_\theta^1 \frac{\omega}{\omega-1} \cdot (1-\theta)^{\omega-1} \theta^{-\omega n}\left[1 + \frac{\omega-1}{\omega} \cdot n \cdot \frac{1-\theta}{\theta}\right] d\theta \tag{17}$$

giving the steady state temperature distribution in the inverse form $z = z(\theta; n, \omega)$ for any value of n and for $\omega = 2,5$. Results are shown in Fig. 5 for the cases $n = 2,3,4,5,6$. Solid curves pertain to laminar boundary layer flow, whereas dashed contours correspond to turbulent boundary layer flow. It should be remarked that if one had neglected the effect of $T_w(x)$ on the local heat transfer coefficient Nu(x) then laminar and turbulent results would be identical in these coodinates. While the difference does not appear too impressive in Fig. 5, it is amplified in calculating the local rate of radiative transfer (normalized by the value at the leading edge), i.e. $\eta \equiv \theta^n$. This is shown in Fig. 6 for the special case $n = 4$ (constant emissivity). Laminar boundary layer results for the case $n = 4$ compare very favorably with the exact solution (for $Pr \to \infty$) given by Lighthill (9), with departures not

exceeding 0.17 percent over the limited range of z covered by Lighthill's power-series expansions. As suggested by Fig. 4, still better agreement would be expected in the turbulent case, since heat transfer coefficients are then less sensitive to surface temperature variations.

Of particular interest is the overall rate of radiative transfer for the entire surface [cf. Eq. (18)]. This is conveniently described in terms of a nondimensional coefficient, $\bar{\eta}$, defined as follows

$$\bar{\eta} \equiv \frac{\int_0^L \epsilon_w \sigma T_w^4 \, dx}{\epsilon_w(T_e) \cdot \sigma T_e^4} \tag{18}$$

This quantity has the character of a radiative "fin efficiency" (26). When expressed in terms of the dimensionless variables θ, z, $\mathcal{R}$, one finds

$$\bar{\eta} = \mathcal{R}^{-\omega} \int_0^{\mathcal{R}} [\theta(z;n)]^n \omega z^{\omega-1} dz \tag{19}$$

But an expression for $\omega z^{\omega-1} dz$ in terms of θ alone is readily obtained from Eq. (17) so that term-by-term integration is possible. One thus obtains the remarkably simple result

$$\bar{\eta} = \frac{\omega}{\omega-1} \left(\frac{1-\theta}{z\theta^n} \right)^{\omega} \cdot \theta^n \tag{20}$$

where, in this case, θ and z are evaluated at the trailing edge ($z = \mathcal{R}$). Results for the integrated radiation effectiveness factor are collected in Fig. 8 where the absicca is not $\mathcal{R}$ but rather

$$\bar{\mathcal{R}} \equiv \frac{\omega-1}{\omega} \mathcal{R} \tag{21}$$

With this choice of absicca, it is seen that laminar and turbulent results are almost coincident for each value of the parameter n. The parameter $\bar{\bar{\mathcal{R}}}$ is merely a dimensionless radiation parameter identical to $\mathcal{R}$ [cf. Eq. (14)] but based on the global heat transfer coefficient $\overline{Nu}_{iso}$ rather than $Nu_{iso}(L)$.

We are now in a position to make an interesting comparison between two extreme cases. Imagine two flat plates differing only in their thermal conductivities and placed in identical fluid dynamic environments. In the steady state, which plate will lose more energy by radiation, and thereby extract energy at a greater rate from the fluid? Evidently, this comparison is most readily carried out for the extremes of zero and infinite thermal conductivity. In the latter case, by an <u>overall</u> energy balance, the perfect conductor must assume a <u>uniform</u> temperature given by the solution of the algebraic equation

$$\bar{\bar{\mathcal{R}}} \cdot \theta^{n} = 1 - \theta \qquad (22)$$

The relevant radiation effectiveness factor $\bar{\eta}$ would then be computed from θ^n. When this comparison is made one obtains a very intriguing result; <u>viz</u>. while the <u>insulating plate always radiates away more energy than the conducting plate, the difference is extremely small for all values of the radiation parameter $\bar{\bar{\mathcal{R}}}$</u>. For constant emissivity flat plates the difference never exceeds 2½ percent in the laminar case (attained at $\bar{\bar{\mathcal{R}}} \approx 1.2$) or 0.27 percent in the turbulent case (attained at $\bar{\bar{\mathcal{R}}} \approx 1.5$). Moreover, this difference will decrease as n increases so that, for practical purposes, it may be said that metals of either zero or infinite thermal conductivity would radiate away equal amounts of energy per unit time.

Of course, in practice, a very important difference in these two cases is the existence of very high surface temperatures, and gradients, in the leading edge region of insulating surfaces. This may, for instance, cause local melting of a low conductivity plate under conditions for which a plate of much larger thermal conductivity would remain intact. However, two comments should be made about the leading

edge region in view of the approximations inherent in the theory. First, as pointed out by Lighthill (9), the infinite gradients appearing at $x = 0$ are a consequence of the predicted behavior of the boundary layer thickness $\delta_{iso}(x)$ as $x \to 0$. This behavior is incorrectly given by boundary layer theory so that the surface temperatures $\theta(z;n)$ indicated in Fig. 5 for $z \to 0$ will in fact be rounded off at a somewhat lower value.* Lighthill estimated this effect by noting that the boundary layer at $x = 0$ can be regarded as being of finite thickness, or order ν/u_e for $Pr = O(1)$. Balancing the heat input $\lambda[T_e - T_w(+0)]u_e/\nu$ against the radiation loss $\epsilon_w \sigma[T_w(+0)]^4$ gives an equation for $\theta(0)$ of the form (22) but with $\bar{\mathcal{R}}$ replaced by

$$\frac{\epsilon_w(T_e)\cdot\sigma T_e^4}{\lambda T_e u_e/\nu} \tag{23}$$

Consequently, when this parameter is small, we have

$$\theta(0) \sim 1 - \frac{\epsilon_w(T_e)\cdot\sigma T_e^4}{\lambda T_e u_e/\nu} \tag{24}$$

Second, owing to the large gradients occurring near the leading edge, longitudinal heat conduction would be expected to play some role in reducing the actual temperature in this region. But, since the nondimensional parameter

$$\frac{\lambda'}{\lambda}\cdot\frac{t}{L}\cdot\frac{1}{\overline{Nu}_{iso}} \tag{25}$$

is frequently very small (where λ' is the thermal conductivity of the solid and t is its thickness in the leading edge region), this suggests that the effects of finite material conductivity will be confined to a leading edge "boundary layer" (within the material) of <u>axial</u> extent

*Of course, for blunted shapes $\delta_{iso}(0)$ is finite so that $\theta(0)$ can be considerably less than unity (cf. Section 3.3).

$$\delta' \sim L \left\{ 2 \frac{\lambda'}{\lambda} \frac{t}{L} \cdot \frac{1}{\overline{Nu}_{iso}} \right\}^{2/3} \tag{26}$$

Thus, conduction alone would be expected to cause $\bar{\theta}(0)$ to differ from unity by an amount proportional to the small parameter given in Eq. (25). Returning to the radiation cooling/catalytic surface reaction analogy, the first of these effects (i.e. breakdown of boundary layer theory) will also be applicable for catalysts with sharp leading edges; however, the correction for axial diffusion along the solid is negligible. With these restrictions in mind we may then conclude this section with a synopsis of the analogy and a brief statement of the accuracy of computing $T_w(x)$ using local values of the isothermal heat transfer coefficient $Nu_{iso}(x)$.

Table 2 summarizes the radiation cooling/catalytic surface reaction analogy for laminar or fully turbulent boundary layers developing along a flat plate. It is seen that the analog of $\mathcal{R}$ in the catalysis problem is the nondimensional catalytic parameter (27, 28)

$$\mathcal{C} \equiv \frac{k_w \cdot (\rho \alpha_e)^n}{Nu_{D,iso}(L) \cdot D \rho \alpha_e / L} \tag{27}$$

which compares the characteristic rate of reaction (numerator) to the characteristic rate of reactant diffusion (denominator). In the diffusion-reaction case the Nusselt number Nu_{iso} is not numerically equal to the heat transfer coefficient but can be obtained from it by making the parameter replacement: $Pr_\lambda \rightarrow Pr_D$. Here $Pr_D (\equiv \mathcal{D}/D)$ is the diffusional Prandtl number.* The nondimensional transfer coefficients ϕ and $\bar{\phi}$ introduced in Table 2 may be used in place of η, $\bar{\eta}$ in some applications. For instance, $\bar{\phi}$ compares the actual rate of radiative transfer with the total convected

*In the Western chemical engineering literature $Nu_{iso}(Re, Pr_D)$ is usually called the Sherwood number and Pr_D is called the Schmidt number.

rate at which heat would have to be removed to maintain the plate at a temperature which is negligible by comparison with T_e. The coefficients $\bar{\eta}$ and $\bar{\Phi}$ are clearly related, in fact

$$\bar{\mathcal{R}}\,\bar{\eta} = \bar{\phi} \tag{28}$$

It may be verified that each of the curves shown in Fig. 7 has the property $\bar{\eta} \sim \bar{\mathcal{R}}^{-1}$ for large $\bar{\mathcal{R}}$ showing that, in this extreme, $\bar{\Phi} \to 1$. Again, by analogy with the diffusion-surface reaction case, it is conceivable that the theoretical relations discussed in this section could be used to experimentally infer total hemispheric-emissivities. Such an application would be akin to the measurement technique described in Ref. (29) where the steady state temperature distribution in a radiating fin is used to obtain its surface emissivity.

While it can be shown that the local application of $Nu_{iso}(x)$ will always underestimate the actual local surface temperature,* the magnitude of this effect is relatively small, especially for turbulent boundary layers with $\underline{n} > 4$ (i.e. metals). However, for laminar boundary layers developing along radiating solids with $\underline{n} \approx 2$ (ceramics) the errors can reach six percent for $Pr = O(1)$ and exceed this value for small Prandtl numbers. It can also be shown (30) that the errors incurred for flat plates cannot be exceeded in the presence of non-zero pressure gradients (e.g. wedge flows). Therefore, in most practical applications, local application of isothermal heat transfer coefficients should result in adequate surface temperature predictions.

2.3 Extension to High Mach Numbers (9)

For the case of laminar flow over a flat plate at low Mach numbers, viscous dissipation of kinetic energy begins to modify the steady state temperature profile

*and, hence, the total rate of radiation loss.

before significantly altering the fluid properties. Pohlhausen (31) showed that, in the absence of heat transfer, the surface temperature would then achieve a uniform value, T_r, which is, in general, higher than T_e and different from the mainstream total temperature

$$T^o \equiv T_e + \tfrac{1}{2} u_e^2 / c_p \tag{29}$$

By numerically solving a generalized form of Eq. (4), viz.

$$u\frac{\partial T}{\partial x} + v\frac{\partial T}{\partial y} = \frac{\nu}{Pr_\lambda}\frac{\partial^2 T}{\partial y^2} + \frac{\nu}{c_p}\left(\frac{\partial u}{\partial y}\right)^2 \tag{30}$$

the recovery temperature was found to be given by an expression of the form

$$T_r = T_e + r_\nu(Pr_\lambda)\cdot\frac{\tfrac{1}{2}u_e^2}{c_p} \tag{31}$$

where the recovery factor $r_\nu(Pr_\lambda)$ is well represented by $(Pr_\lambda)^{\frac{1}{2}}$ for values of the Prandtl number not very different from unity. Owing to the linearity of Eq. (30), solutions of the homogeneous energy equation (4) can be added to this special solution of the inhomogeneous equation (30) and still satisfy Eq. (30). Thus, heat transfer in the presence of viscous dissipation can be calculated using $M_\infty = 0$ heat transfer coefficients by merely replacing the mainstream fluid temperature, T_e, with the recovery temperature T_r[cf. Eq. (31)]. At still larger Mach numbers the thermal properties of the fluid can no longer be considered constant, but for air the variation of the nondimensional group $Pr_\lambda \equiv c_p\mu/\lambda$ is minor compared with variations in such individual properties as the dynamic viscosity μ and local density ρ. This fact, coupled with the observation that only the temperature insensitive product $\rho\mu$ centers directly into the transformed compressible boundary layer equations, led Chapman and Rubesin (32) to the conclusion that for any $T_w(x)$, the temperature field within the boundary layer would bear the same relation to x and the stream function

ψ as in the low Mach number case. Consequently, except for a small correction to the heat transfer coefficient Nu accounting for variable $\rho\mu$, the procedure outlined above for small Mach numbers becomes approximately valid for arbitrary Mach number.* Turning to the radiation cooling problem at hand this implies that all previous results for $\omega = 2$ (laminar boundary layer flow) can be extended to the compressible case by (i) replacing the stream temperature T_e wherever it appears with the recovery temperature T_r and (ii) correcting the heat transfer coefficient $Nu_{iso}(L)$ for the variability of $\rho\mu$. This procedure should lead to accurate results provided the latter correction is not large.† However, if it is large then the basic relation between the local heat transfer coefficient and $T_w(x)$ must first be generalized to account for streamwise variations in the $\rho\mu$ correction (or reference temperature; cf. footnote below). To the writer's knowledge this has never been carried through, although thhe problem is far from intractable.‡

While the theoretical justification becomes weaker, similar comments can be made for the turbulent boundary layer case; i.e. to extend $\omega = 5$ results of Section 2.2 to the compressible case replace T_e everywhere by the turbulent recovery temperature and correct $Nu_{iso}(L)$ for variable properties using the reference temperature method

---

*subject to the limitation that $Pr_\lambda \approx$ const.

†this correction can only be arrived at by comparison with exact solutions or experiment. For practical applications the Rubesin-Eckert reference temperature method has been found to be convenient in a wide variety of circumstances (33,34).

‡for example, methods similar to those recently applied by Mayer (35) could be used for generalizing Eq. (11) to account for streamwise variations in reference temperature. Since the latter will be expressible in terms of θ itself, the remainder of the calculation would proceed as in Section 2.2

(or an equivalent method). In this case it should be anticipated that the variable property correction will quickly dominate the isolated effect of variable surface temperature [or $\vartheta_e(x)$] on Nu (cf. Fig. 4). This should allow the use of calculation methods which completely ignore the surface temperature "history" effect accounted for in Section 2.2. In unusual circumstances, however, the accuracy of such predictions is questionable (an example might be in the immediate neighborhood of an abrupt change in surface emissivity). Here again, these areas remain largely unexplored.*

Summarizing then, in a chemically inert high speed stream, radiation losses will prevent most of the surface of an immersed, insulating solid from reaching the gasdynamic recovery temperature T_r. According to continuum boundary layer theory, however, the leading edge region of sharp-nosed bodies will seek the full recovery temperature. While local breakdown of boundary layer theory and internal heat conduction modify this conclusion somewhat (cf. Section 2.2) these effects only slightly increase the flight Mach number beyond which localized material degradation may be expected. But for particular applications in which localzed failure can be prevented (say, by moderate blunting) one has, in radiation cooling, the possibility of a relatively simple and efficient heat protection scheme. Of course for long duration trajectories this implies the existence of (i) effective means for insulating the radiating vehicle skin from the underlying structure and payload; and (ii) adequate means for sustaining aerodynamic and aerothermoelastic loads acting directly

---

* an analagous situation exists in the case of chemical surface reactions when the catalytic activity undergoes abrupt streamwise variations. Several such cases have been quantitatively investigated by Chung, Liu and Mirels (36). A qualitative discussion of this general problem may be found in Ref. (27).

on the vehicle skin. Further complication arises from the fact that current temperature limitations on refractory metal coatings* renders the use of ceramic leading edges and nose caps more likely.† As will be seen, some of these ceramic nose and leading edge materials can operate at temperature levels sufficient to dissociate oxygen molecules at realistic stagnation pressures. With this in mind, it is then of interest to examine the radiation cooling of solids in the presence of thermochemical change.

*available coatings to protect refractory metals from catastrophic oxidation rates fail at temperatures well below the melting points of the metals themselves.

†Thus, the case of precewise discontinuous emissivity alluded to earlier is of more than academic interest.

3. THERMOCHEMICAL EFFECTS IN RADIATION COOLING

In the previous section radiation cooling and chemical surface catalysis were presented as analogous but separate problems. Moreover, the thermal effects which accompany most chemical reactions were suppressed by considering only <u>isothermal</u> catalyst surfaces with $T_w = T_e$. But if the surface reaction is exothermic, in order to prevent increases in the surface temperature one must remove energy continuously (say, by internal cooling). In the absence of such cooling the surface temperature would rise until, at each point, heat loss by convection (to the cooler stream) and by radiation ($\epsilon_w \sigma T_w^4$) balanced the heat $\dot{R}''Q$ generated per unit catalyst area in the chemical surface reaction.

3.1 <u>Generalization of the Recovery Temperature Concept</u> (<u>37-40</u>)

Consider first the extreme case of negligible radiation loss from a catalyst of extremely great activity ($k_w \to \infty$) in a low speed stream. One then finds that the catalyst will settle out at a temperature which is, in general, higher* than T_e and different from the mainstream "total" temperature

$$T^\circ \equiv T_e + \frac{\alpha_e Q}{c_p} \tag{32}$$

For laminar boundary layer flow this catalyst "recovery" temperature is found to be

$$T_r \equiv T_e + r_D(Pr_\lambda, Pr_D) \cdot \frac{\alpha_e Q}{c_p} \tag{33}$$

---

*when the heat, Q, released per unit mass of transformed reactant is positive

where, by analogy with the nonreactive problem discussed in Section 2.3, the function $r_D(Pr_\lambda, Pr_D)$ may be called the recovery factor for free stream chemical energy (38). Explicitly, r_D is given by*

$$r_D \equiv \frac{Pr_\lambda}{Pr_D} \cdot \frac{Nu_{D,iso}}{Nu_{\lambda,iso}} \approx (Le)^{2/3} \tag{34}$$

[the last (approximate) equality following from Pohlhausen's observation (31) that $Nu_{iso} \sim Pr^{1/3}$ for $Pr = O(1)$.] When the mainstream contains both kinetic energy ($\frac{1}{2} u_e^2$ per unit mass) and chemical energy ($\alpha_e Q$ per unit mass of mixture), one then anticipates the combined result

$$T_r' \equiv T_e + r_\lambda \cdot \frac{\frac{1}{2} u_e^2}{c_p} + f_D \cdot \frac{\alpha_e Q}{c_p} \tag{35}$$

which has, in fact, been derived by Vaulin (37) for the special case of compressible laminar flow over a flat plate. Thus, only when the surface temperature T_w has the value T_r' given by Eq.(35) does the net energy flux to the plate vanish. If the plate is radiating energy to its surroundings, this energy must be derived from the main stream. It follows that for any $x > 0$ radiation loss will cause the plate

*The consequences of these relations for the recovery temperature [cf. Eqs.(31,33)] are somewhat startling when $Pr_\lambda > 1$, $Le > 1$ (28,38). For pure gases like water vapor, the recovery temperature exceeds the thermodynamic total temperature of the gas stream. Similarly, when $Le > 1$ (as in the case of weakly dissociated diatomic gases), the steady state surface temperature exceeds the thermodynamic total temperature.

temperature $\bar{T}_w$ to fall below the generalized recovery temperature $\bar{T}'_r$. An argument paralleling that given in Section 2.3 reveals that the law governing this temperature decay, $\bar{T}_w(x)$, would be precisely that given for the incompressible, nonreactive radiation cooling problem (cf. Section 2.2) provided one replaced $\bar{T}_e$ by $\bar{T}'_r$ and corrected the heat transfer coefficient $Nu(x)_{iso}$ for fluid property variations. Thus

$$\bar{T}_w(x) = \bar{T}_r' \cdot \theta(\mathcal{Z}; n) \tag{36}$$

where

$$\mathcal{Z} = \frac{\epsilon_w(\bar{T}_r') \cdot \sigma \bar{T}_r'^4}{\lambda \bar{T}_r' / \delta_{iso}(x)} \tag{37}$$

3.2 Effects of Finite Catalyst Activity

The problem becomes considerably more complex if due account is taken of the finite catalytic activity of real surfaces. Then, even in the absence of radiation loss a nontrivial distribution of surface temperature results.* In particular, $\bar{T}_w(0)$ attains the (nonreactive) gas dynamic recovery temperature $\bar{T}_r$ and $\bar{T}_w(\infty)$ attains the generalized recovery temperature $\bar{T}'_r$. If the chemical rate constant k_w has a temperature dependence of the two-parameter Arrhenius form

$$k_w = A \exp\left[-E/(R\bar{T}_w)\right] \tag{38}$$

then, for a prescribed reaction order, the surface temperature distribution $\bar{T}_w(x)$ will depend upon the activation energy parameter $E/(R\bar{T}_r)$ as well as the catalytic parameter† $\mathcal{C}$ of Section 2.2. Qualitatively, exothermic surface reaction does not cause the leading edge temperature $\bar{T}_w(0)$ to rise above $\bar{T}_r$ because of the excellent

---

*except when internal-heat conduction renders the surface temperature constant, thereby allowing isothermal catalysis solutions to be applied to the radiation cooling problem with exothermic surface reaction.

†The rate constant k_w appearing in the definition of the catalytic parameter $\mathcal{C}$ is to be evaluated at the gasdynamic recovery temperature [cf. Eq. (31)].

conditions of heat removal in this region. Further downstream, however, the temperature is able to rise above $\bar{T}_r$ and this is accompanied by a corresponding increase in the reaction rate coefficient [cf. Eq. (38)]. Very far downstream the steady state rate of heat evolution (and hence heat removal) becomes diffusion limited so that the surface temperature approaches $\bar{T}_r'$ asymptotically. But this latter condition would not be achieved in the presence of radiation heat loss, for then it is readily shown that $\bar{T}_w$ vanishes as $\chi \to \infty$ in accord with the asymptotic behaviour*

$$\frac{\bar{T}_w}{\bar{T}_r} \sim \left\{ \frac{1 + r_D \alpha_e Q/(c_p \bar{T}_r)}{z} \right\}^{1/n} \tag{39}$$

When compared with the corresponding result in the absence of the chemical contribution, Eq. (39) reveals that the addition of chemical energy to the free stream would increase catalyst surface temperatures very far downstream by the factor

$$\left\{ 1 + r_D \frac{\alpha_e Q}{c_p \bar{T}_r} \right\}^{1/n} \tag{40}$$

Apart from mentioning these general features, we shall not dwell on this coupled radiation cooling-catalysis problem further,† but instead turn to a simpler but perhaps more practical example which exhibits similar features. Consider, the case of radiation-cooled blunt leading edges or nose caps, again within the framework

---

*here z and n are defined by Eqs. (15) and (2), respectively. In Eq. (14) T_e is replaced by T_r.

†a detailed investigation of this particular problem is, in fact, nonexistent.

of boundary layer theory. Here, in the usual situation atomic oxygen and nitrogen represent the chemical energy content of the gas at the outer edge of the boundary layer and first order (n = 1) heterogeneous recombination is the exothermic surface reaction of interest (42-44).* Except for certain extreme flight conditions† or test conditions,‡ atomic oxygen is usually absent in the undisturbed medium but is formed behind bow shock waves at a finite rate. If $\bar{V}_\infty$ is the effective flight velocity then, the energy equation applied between upstream infinity (subscript ∞) and the forward stagnation point (subscript e) provides the relation

$$\frac{1}{2}\bar{V}_\infty^2 + c_{p,\infty}\bar{T}_\infty = c_{p,e}\bar{T}_e + \alpha_e Q \qquad (41)$$

Thus, for a given flight condition, the static temperature, $\bar{T}_e$, at the outer edge of the boundary layer decreases with increasing local atom concentration. To understand the effects of thermochemical change on the surface temperatures of such radiation cooled solids one must then account for the fact that the chemical contribution to the enthalpy makes its appearance only at the expense of the thermal contribution. It may also be necessary to account for the property that a sufficiently hot surface can dissociate incident molecules as well as recombine incident atoms (23,42). The dominant effects of these phenomena are readily perceived using the following simple model.

3.3 Radiation Cooled Stagnation Region with Shock Layer Dissociation (4)

The steady state temperature of a nose cap will, as before, be the temperature at which the radiation term $\epsilon_w \sigma \bar{T}_w^4$ balances the aerodynamic heat flux. When

---

*only nonablating surfaces are considered here.

†corresponding to photodissociation or predissociation caused say, by a nuclear blast (45,46).

‡corresponding to recombination nonequilibrium in shock tunnel nozzles (47).

the gas at the outer edge of the boundary layer is partially dissociated the input heat flux due to convective processes within the boundary layer may be represented as the sum of two contributions, $\dot{q}''_\lambda$ and $\dot{q}''_D$. Here $\dot{q}''_D$ represents the contribution due to thermochemical changes across the gas phase boundary layer. When all of the reaction occurs at the gas/solid interface,* each of these contributions may be expressed in terms of its nondimensional transfer coefficient (Stanton number) and driving force as follows (40)

$$\dot{q}''_\lambda = St_\lambda \cdot \rho_e u_e \bar{c}_p \cdot (T_r - T_w) \tag{42}$$

$$\dot{q}''_D = St_D \cdot \rho_e u_e \cdot (\alpha_e - \alpha_w) Q \tag{43}$$

where T_r represents the gas-dynamic recovery temperature,† α represents the mass fraction of atoms present in the partially dissociated mixture, and Q is the heat of atom recombination (assumed constant). The remaining symbols and subscripts are defined in the nomenclature.

With these preliminary statements in mind the steady state heat balance equation may be written

$$\epsilon_w \sigma T_w^4 = St_\lambda \rho_e u_e \bar{c}_p \cdot (T_r - T_w) + St_D \rho_e u_e \cdot (\alpha_e - \alpha_w) Q \tag{44}$$

At this point it is convenient to introduce the following notation.

$$T_e^\circ \equiv T_e + \tfrac{1}{2} u_e^2 / \bar{c}_p + \alpha_e Q / \bar{c}_p \tag{45}$$

---

*The conditions under which this assumption is valid will be explored in Section 3.4. The case of local thermochemical equilibrium within the boundary layer will be approximately equivalent to a special case ($\mathcal{C} = \infty$) treated here.

†At the forward stagnation point the kinetic energy term $\frac{1}{2}u_e^2$ vanishes so that $T_r = T_e$ regardless of the magnitude of the Prandtl number$^{\frac{2}{3}}$ Pr_λ. Despite the fact that $\rho_e u_e \to 0$ the product $St \cdot \rho_e u_e$ is finite.

$$r_D \equiv St_D / St_\lambda \tag{46}$$

$$\phi \equiv (\alpha_e - \alpha_w) / \alpha_e \tag{47}$$

At any point in the flow field the quantity $\bar{T}^o$ will be recognized as the static temperature which would be attained locally if the kinetic energy $\frac{1}{2}u^2$ and the chemical energy a Q were adiabatically converted into sensible temperature rise. The quantity r_D, being a ratio of transfer coefficients (St) for mass and heat, may be regarded as the recovery factor for chemical energy and will be different from unity if the Lewis number Le for atom diffusion through the mixture is different from unity. Lastly, the coefficient ϕ is a measure of the depletion of atoms across the boundary layer due to chemical change. In terms of these quantities Eq. (44) becomes

$$\epsilon_w \sigma T_w^4 = St_\lambda \cdot \rho_e u_e \cdot \bar{c}_p \cdot \left\{ (\bar{T}_e^o - T_w) + (r_D \phi - 1)(\alpha_e Q / \bar{c}_p) \right\} \tag{48}$$

Now imagine the same surface element in a gaseous environment which does not dissociate. This condition will be designated hereafter by the subscript I, for "inert". In the "inert" case, if the flight speed and other properties of the medium are unchanged, the surface temperature $T_{w,I}$ will satisfy the simplified heat balance equation:

$$\epsilon_w \sigma T_{w,I}^4 = St_\lambda \cdot \rho_e u_e \cdot \bar{c}_p (T_e^o - T_{w,I}) \tag{49}$$

where the quantities $St_\lambda \rho_e u_e$, $\bar{c}_p$ and T_e^o will be approximately equal to those appearing in Eq. (48). Identification of the "total" temperature T_e^o is, in fact, a consequence of energy conservation; i.e., the stagnation enthalpy of the gas with respect to the vehicle should be the same in both cases. Hereafter, the common "total" temperature T_e^o will be designated T^o. It will also prove convenient to

define the following dimensionless temperature ratios:

$$\theta \equiv T_w / T^\circ \tag{50}$$

$$\theta_* \equiv 1 + \left[r_D \phi - 1 \right] \frac{\alpha_e Q}{\bar{c}_p T^\circ} \tag{51}$$

$$\theta_I \equiv T_{w,I} / T^\circ \tag{52}$$

and a convection-radiation parameter of the form defined by Eq. (14), viz.

$$\mathcal{R} \equiv \frac{\epsilon_w (T^\circ) \cdot \sigma \cdot (T^\circ)^4}{St_\lambda \rho_e u_e \cdot \bar{c}_p T^\circ} \tag{53}$$

From the defining relation for the surface temperature $T_{w,I}$, we then have the familiar n^{th}-degree algebraic equation for θ_I ($\mathcal{R}$)

$$\mathcal{R} \theta^n = 1 - \theta \tag{54}$$

Similarly Eq. (48) takes the more general form

$$\mathcal{R} \theta^n = \theta_* - \theta \tag{55}$$

which reduces to Eq. (54) only when $\theta_* = 1$.

When the convection-radiation parameter $\mathcal{R}$ vanishes Eq. (54) shows that θ_I achieves its maximum value of unity. Thus the total temperature T° is seen to be the maximum value of the surface temperature for motion through an inert atmosphere. Similarly, when $\mathcal{R} \to 0$ then $\theta = T_w/T^\circ$ attains the value θ_* in a dissociating atmosphere. It is seen from Eqs. (54) and (55) that the new temperature variable $\tau = \theta/\theta_*$ will satisfy the same algebraic equation as θ_I if the convection-radiation

parameter $\mathcal{R}$ is replaced by $\Theta_*^{n-1}\mathcal{R}$; i.e.:

$$(\Theta_*^{n-1}\mathcal{R})\cdot\tau^n = 1-\tau \tag{56}$$

For n = 4 Fig. 8 shows a plot of the reduced temperature $\tau = \Theta/\Theta_*$ against the modified radiation parameter $\Theta_*^3\mathcal{R}$. The cube root of this parameter (i.e., $\Theta_*\mathcal{R}^{1/3}$) may be given an alternative interpretation as follows. $\mathcal{R}^{1/3}$ itself can be considered to be the ratio of the total temperature T^o to a characteristic convection-radiation temperature T_ϵ defined by (9)

$$T_\epsilon = \left\{ St_\lambda \rho_e u_e \bar{c}_p / (\epsilon_w \sigma) \right\}^{1/3} \tag{57}$$

Thus, the parameter $\Theta_*\mathcal{R}^{1/3}$ is equivalent to the grouping:

$$(T^o/T_\epsilon)\left\{1 + [r_D\phi - 1][\alpha_e\psi/(\bar{c}_p T^o)]\right\} \tag{58}$$

Equations (54) and (55) reveal that Θ can actually exceed Θ_I provided the characteristic temperature ratio Θ_* defined by Eq. (51), exceeds unity. This might be called a temperature "overshoot" since the surface temperature T_w would then actually exceed that attained in an inert atmosphere at the same velocity (V_∞) and density (ρ_∞). Since an overshoot is impossible when $\Theta_* < 1$ the quantity Θ_* plays the role of a discriminant. If this discriminant were rigorously constant then the extent of the temperature overshoot could not exceed that achieved in the absence of radiation loss ($\mathcal{R} \Rightarrow 0$). In practice, however, Θ_* will itself be a function of the surface temperature Θ and hence, implicitly, a function of the convection-radiation parameter $\mathcal{R}$. Qualitatively speaking, the nature of this dependence usually makes an overshoot impossible when $\mathcal{R} = 0$ but possible for large values of $\mathcal{R}$ provided the surface is an active catalyst for atom recombination and the average Lewis number for atom diffusion exceeds unity.

This can be seen as follows (4). In the absence of gas phase chemical reaction, the rate of convective diffusion of atoms to the gas/solid interface must be

identically equal to the net interfacial rate of atom recombination. Owing to the possibility of dissociation at the radiating surface the net rate of atom recombination must be written (23,42)

$$\dot{\mathcal{R}}'' = m_1 \cdot k_w(T_w) \cdot \{ n_{1,w} - n_{1,eq}(T_w ; p) \} \tag{59}$$

where the rate constant k_w is related to the recombination coefficient* γ and atomic mass m_1 by (23,43)

$$k_w = \{ kT_w / (2\pi m_1) \}^{1/2} \cdot \gamma(T_w) \tag{60}$$

If the local atom number density n_1 is replaced by the atom mass fraction, α, the atom conservation equation at the gas/solid interface becomes

$$St_D \cdot \rho_e u_e \cdot (\alpha_e - \alpha_w) = k_w \rho_w \left\{ \alpha_w - \alpha_{eq}(\theta) \left[\frac{1+\alpha_w}{1+\alpha_{eq}(\theta)} \right] \right\} \tag{61}$$

Defining a non-dimensional catalytic parameter $\mathcal{C} \equiv k_w \rho_w / [St_D \rho_e u_e]$ and solving for $\phi \equiv (\alpha_e - \alpha_w)/\alpha_e$ we find (4):

$$\phi(\theta) = \frac{\mathcal{C}(\theta)}{1 + \mathcal{C}(\theta) + \alpha_{eq}(\theta)} \left[1 - \frac{\alpha_{eq}(\theta)}{\alpha_e} \right] \tag{62}$$

where both $\mathcal{C}$ and $\alpha_{eq}(T_w; p)$ can be strong functions of the surface temperature† T_w.

As the dimensionless surface temperature Θ decreases (with increased radiation loss) it is seen that $\alpha_{eq}(\Theta)$ will eventually become negligible compared to α_e and,

---

*If the recombination reaction is truly first order (n = 1) then the recombination coefficient γ for a particular surface will depend on surface temperature alone.

†effects of this temperature dependence will be discussed further in Section 3.5.

ipso facto, negligible compared to unity. In this extreme, we have the familiar result (38,43,44) for the extent of recombination:

$$\phi \rightarrow \frac{\mathcal{C}}{1+\mathcal{C}} \tag{63}$$

On the other hand, if we consider the stagnation region with the atom concentration α_e at equilibrium with the local temperature T_e it is apparent that ϕ will vanish when $T_w = T_e$ since, in this case, $\alpha_{eq}(T_w) = \alpha_e$ regardless of the magnitude of $\mathcal{C}$. Thus, we have a realistic situation for which, in the absence of radiation loss, there can be no temperature over-shoot even for a "perfect" catalyst (i.e., even for $\mathcal{C} \gg 1$). This high temperature behaviour of the extent of recombination, ϕ, is illustrated in Fig. 9 for the case of partially dissociated hydrogen at a pressure of 0.1 atm. and real gas stagnation temperature of 3000°K.* The combined effects of surface reaction and radiation loss on the steady state temperature of a constant emissivity solid are illustrated in Fig. 10, again for the case of equilibrium hydrogen ($T_e = 3000°K$; $P_e = 0.1$ atm). Here contours of constant surface temperature are shown on the log $\mathcal{C}$-log $\mathcal{R}$ plane together with a (shaded) domain within which the surface temperature is actually higher than it would have been in the absence of dissociation. This overshoot occurs only for active catalysts if the recovery factor r_D exceeds unity† and radiation loss ($\mathcal{R}$) is sufficient to depress the surface temperature T_w to the extent that the corresponding equilibrium degree of dissociation $\alpha_{eq}(T_w)$ becomes small compared to the atom concentration α_e established at the outer edge of the

*While $\mathcal{C}$ is taken to be the parameter, it should be remembered that, for any particular surface, $\mathcal{C}$ will itself vary as the surface temperature is reduced.

†Recent transport property estimates (48) indicate that the Lewis number for weakly dissociated hydrogen at 3000°K is about 1.65. This would imply $r_D \approx 1.35$.

boundary layer. On most of the log $\mathcal{C}$ - log $\mathcal{R}$ plane surface temperatures are considerably lower than they would have been in the absence of dissociation, as reflected by the positive slope of $\bar{T}_w \equiv$ const. contours outside the shaded region. At point P, for example, the difference amounts to about 250°K. The straight line of unit slope* passing through point P represents the locus of operating points under a contemplated change in scale alone. Under such a change, the positive slope of $\bar{T}_w =$ const. contours indicates that the equilibrium surface temperature will change by a smaller amount than in the nondissociated case; a characteristic which will be explored more fully in Section 3.4.

Simple considerations such as those presented above allow one to single out the important physicochemical parameters governing this class of radiation-cooling phenomena. It is then possible to estimate the magnitude of these nondimensional parameters ($\mathcal{R}, \mathcal{C}, \theta_*$) as encountered in high speed motion through the Earth's atmosphere by collectively drawing in the work of Refs. 43,49,50. A convenient representation is obtained by constructing contours (level lines) of constant $\mathcal{R}, \mathcal{C}, \theta_*$ on the altitude-velocity plane, on which typical re-entry trajectories can be superimposed. Three such contour maps are shown in Figs. 11, 12, 13, each of which contains the re-entry trajectory† of a typical satellite (51) (marked S) and boost glide vehicle (52) (marked BGV). The point on each trajectory at which the product $\rho_\infty^{0.5} V_\infty^{3.15}$ passes through a maximum is marked with an open circle (this would be the point of peak convective heat input, $\dot{q}''_{max}$, in the case of complete

---

*increasing scale (nose radius) increases both transfer coefficients St and St_D at equal rates.

†also included in Fig. 11 is a typical intercontinental ballistic missile trajectory (marked ICBM) for which peak heating rates are seen to be from 1 to 2 orders of magnitude greater than in the case of glide vehicle or satellite re-entry.

atom recombination with $r_D \approx 1$). Also included are dashed contours of constant maximum laminar convective heat flux (in BTU/ft^2-sec.) to a strongly cooled surface of 1 foot nose radius, as calculated from the Detra-Hidalgo correlation (49).

Figure 11 shows the convection-radiation parameter $\mathcal{R}$ [cf. Eq. (53)] for a nose radius of 1 ft. with a surface emissivity of 0.5*. It is seen that during re-entry $\mathcal{R}$ decreases from very large values [of order 10^5 at satellite velocity] to values of order 10^{-1} at slightly supersonic velocities, with peak aerodynamic heat input occurring at $\mathcal{R} = O(10^4)$. Figure 12, shows contours of constant catalytic parameter† $\mathcal{C}$ derived from the calculations of Goulard (43) for chemically frozen boundary layer flow at 200 and 250 Kft. (with a wall temperature of 700°K). Numerical values on each set of contours also correspond to a body with one-foot nose radius and the recombination coefficient γ has been set at the intermediate value‡ 10^{-2} (thus, in practice, a factor of 10^2 in either direction is possible, depending upon whether the nose material is a very good or very poor atom recombination catalyst.) Contrary to $\mathcal{R}$, the catalytic parameter $\mathcal{C}$ does not change very rapidly along a re-entry trajectory; its absolute value could be anywhere from 10^{-2} to 10^2 depending on the magnitude of the atom recombination coefficient γ. Finally, one requires an estimate of θ_*, or at least its minimum value, since dissociation can reduce the steady state surface temperature appreciably only when $\theta_{*,\,min}$ is less than unity and $\mathcal{C}$ is small (4). Figure 13 gives contours

---

*Since $\mathcal{R} \propto \epsilon_w R_B^{1/2}$ values corresponding to any other nose radius, R_B, or emissivity, ϵ_w, could be constructed from the values given on Fig. 11.

†These contours are marked W = const. anticipating the nomenclature to be adopted in Section 3.4.

‡At any other surface temperature these contours would still be applicable, but to a different γ, in accord with the proportionality $k_w \propto \gamma T_w^{1/2}$ [cf. Eq. (60)].

of constant $1 - [\alpha_s Q/(\bar{c}_p \bar{T}^o)]$, where α_s is the value of α_{eq} computed behind normal shock waves in air. These values, obtained by crossplotting Huber's results for the temperature ratio across normal shocks (50), can be regarded as providing a lower bound to the discriminant Θ_*. It is seen that $\Theta_{*,\,min}$ initially takes on values of about 0.2 (near satellite speed) but rises rapidly to unity near Mach 5. Combining the magnitudes of $\mathcal{R}$ and $\Theta_{*,\,min}$ shown on Figs. 11 and 13, respectively, one finds that the actual wall temperature for the boost-glide vehicle (BGV) entry shown can be lower than that neglecting shock layer dissociation by as much as about 600^oK. This occurs where the noncatalytic wall temperature would be about 1400^oK for the remaining conditions assumed ($\epsilon_w = 0.5$, $R_B = 1$ ft). By the same token $\bar{T}_w$ can be larger than the temperature calculated neglecting heterogeneous atom recombination by some 600^oK. These rough estimates suggest that a low atom recombination coefficient γ for high temperature ceramics (or refractory metal coatings) could play a role comparable to high emissivity in contributing to the success of an overall design.

3.4 Influence of the Aerodynamic Heat Input Law: Dependence on Physical Scale (15)

It has already been demonstrated that the steady state surface temperature of a radiation cooled solid should be less sensitive to contemplated changes in physical dimensions than in the nonreactive case [cf. Section 3.3]. This property can be traced back to the scale dependence of the aerodynamic heat input $\dot{q}''$ since T_w is

always determined from an equation of the form

$$\epsilon_w(T_w)\cdot\sigma T_w^4 \equiv \dot{q}''(T_w) \tag{64}$$

Differentiating this expression with respect to boundary layer thickness,* δ, gives

$$\frac{\partial \ln T_w}{\partial \ln \delta} = \frac{m}{n} \tag{65}$$

where we have written

$$m \equiv \frac{\partial \ln \dot{q}''}{\partial \ln \delta} \tag{66}$$

and, as before

$$n \equiv 4 + d\ln \epsilon_w / d\ln T_w \tag{2}$$

The magnitude of n (i.e. the effect of the emissivity-temperature relation) has already been discussed [cf. Table 1]. The remaining factor influencing is therefore m (i.e. the dependence of input heat flux $\dot{q}''$ on scale). While $m \equiv -1$ for equilibrium boundary layer flow and nonreactive boundary layer flow alike, in general m depends upon chemical kinetic parameters (hence Φ). In the cases treated thus far gas phase recombination has been neglected, i.e. the only chemical kinetic parameter entering the problem was $\mathcal{E}$. The dependence of m on the catalytic parameter is most readily demonstrated for the special case $\alpha_{eq}(T_w) \ll \alpha_e$, for then Eq. (63) implies

$$\frac{\partial \ln \phi}{\partial \ln \mathcal{E}} = 1 - \phi \tag{67}$$

---

*so that the results can be applied to laminar or turbulent boundary layer problems, by later introducing $\delta \propto R_B^{1/2}$ or $\delta \propto R_B^{1/5}$ respectively.

With some manipulation Eqs. (42,53,67) provide the simple result

$$m = -1 + \frac{\phi H}{1+\phi H} \cdot (1-\phi) \tag{68}$$

where we have written

$$H \equiv r_D \frac{[\alpha_e - \alpha_{eq}(T_w)]Q}{\bar{c}_p \cdot (T_e - T_w)} \approx r_D \cdot \frac{\alpha_e Q}{\bar{c}_p (T_e - T_w)} \tag{69}$$

For any prescribed value of this chemical enthalpy potential parameter* H, Eq. (68) shows that m = -1 for either $\psi = 0$ (no recombination) or $\psi = 1$ (complete recombination). But at some intermediate value of ψ the parameter m attains a maximum value, which is, however, less than zero. Simultaneous atom recombination within the boundary layer can cause even larger departures of m from the familiar case of m = -1. While an adequate set of such calculations is not currently available, we can, however, illustrate the nature of this effect by drawing on a simple model for which the complete nonequilibrium solution can be written down in closed form. This is the conductivity cell model (53) depicted in Fig. 14. It is known that such models predict functional dependences which can be applied successfully to many convective flow problems in chemical engineering; indeed this is the basis of so-called film theory. Of course, to carry this analogy through to the computational state a film theory-boundary layer "dictionary" is required, i.e. a set of prescriptions for translating film theory parameters into their corresponding observable quantities for convective heat transfer. For stagnation flow this correspondence may in fact be established by matching film theory predictions with available boundary layer

---

* this parameter may be regarded as the product of the recovery factor r_D and a "chemical Eckert Number". It plays the same role in the theory of heat transfer with chemical reaction as the parameter $r_r \cdot (\frac{1}{2} u_e^2)/[\bar{c}_p \cdot (T_e - T_w)]$ plays in non-reactive compressible boundary layer theory.

solutions in several important limiting cases.*

The continuum model to be used here (cf. Fig. 14) is essentially Broadwell's linearized conductivity cell model (53) but extended to include first order atom recombination at one surface (the "cold boundary") of arbitrary catalytic activity. Thus, we imagine two parallel plates separated by a distance δ, enclosing a layer of partially dissociated diatomic gas. The local atom concentration α is postulated to attain its equilibrium value at the hot plate temperature and, within the cell, thermal diffusion and other secondary transport mechanisms are assumed negligible. For this problem three important nondimensional parameters emerge, written G, W, H. The parameters G and H are precisely those appearing in Broadwell's study, the first of these being a gas phase recombination parameter interpretable as the ratio between the characteristic diffusion time δ^2/D_{12} across the film to the gas phase recombination relaxation time τ. The parameter H, already defined by Eq. (69), is seen to be a measure of the maximum possible chemical enthalpy change $\Delta h_{chem,\,eq.}$ across the cell, as compared to the sensible (frozen) enthalpy change Δh_f corresponding to the imposed temperature difference $\Delta T \equiv T_e - T_w$. The additional kinetic parameter, W, defined by

$$W \equiv k_w \delta / D_{12} \tag{70}$$

is introduced by the finite rate atom recombination at the colder surface.† The special case $W = 0$ corresponds to a completely noncatalytic surface (as treated by

---

*A nonequilibrium Couette flow model of the type investigated in Refs. 53-55 would be required for locations on the body at which viscous dissipation must be accounted for.

†making use of the film theory-boundary layer dictionary, this parameter will be recognized as identical to $\mathcal{C}$. This identity should be kept in mind during the following discussion.

Broadwell) whereas $\bar{W} = \infty$ corresponds to the diffusion controlled ("perfectly" catalytic, $k_w \to \infty$) case. The behavior of the Nusselt number Nu (based on the temperature difference ΔT across the film of thickness δ) is shown in Fig. 15 for the special case $H = 9$, $\alpha_{eq}(T_w) \ll \alpha_e$. Note that Nu approaches $1 + H$ for either large G or large $\bar{W}$, since the extent of recombination Φ is complete in either case. On the other hand, for very small values of G and $\bar{W}$, or for $H \to 0$ the heat transfer coefficient approaches its nonreactive value, unity.

Contours of constant $\bar{W}$ have already been displayed on the altitude-velocity plane (cf. Fig. 11). In a similar way, by drawing on the work of Refs. 52,57 contours of constant G and H may be constructed to provide an overall picture of the nonequilibrium flight regimes to be expected in the earth's atmosphere. Figs. 16 and 17 display this data quantitatively in the range:* $10 < V_\infty < 30$ Kft./sec.; $100 < h < 300$ Kft. Fig. 16 is obtained from a cross plot of Whalen's calculations (52) of the gas phase recombination parameter, and applies to a body of 1 ft. nose radius. Numerical values indicate that lifting vehicles at very high altitudes will most likely experience chemically frozen flow in the boundary layer ($G \to 0$), or the incipient effects of gas phase recombination.† Estimates of the chemical enthalpy potential parameter H shown in Fig. 17 were derived from cross plots of Grier and Sand's calculations (57) of the maximum possible heat flux reduction associated with a completely noncatalytic ($\gamma = 0$) wall.‡ At the point of peak heat transfer to the

---

*outside of this range contours have been sketched in to show only qualitative behavior.

†a tendency which is accentuated at high surface temperatures, (56), such as are likely to prevail in radiation cooling applications.

‡numerical values in this case pertain to the choice $T_w = 1000^\circ$K but H could be larger in practice if high surface temperatures are considered; e.g. order 10 for high temperature ceramics.

boost-glide vehicle (BGV) the heat flux could be reduced by almost a factor of 4. With these magnitudes in mind the effect of the chemical kinetic parameters G and W on the scale dependence parameter m can be estimated using the conductivity cell model, for any prescribed value of H.

Consider a change in scale, or in the case of the conductivity cell model, a change in the film thickness* δ. Then, from the definition of the heat transfer coefficient Nu,

$$m \equiv \frac{\partial \ln \dot{q}''}{\partial \ln \delta} = -1 + \frac{\partial \ln G}{\partial \ln \delta} \cdot \left(\frac{\partial \ln Nu}{\partial \ln G} \right)_W + \frac{\partial \ln W}{\partial \ln \delta} \left(\frac{\partial \ln Nu}{\partial \ln W} \right)_G \tag{71}$$

In view of the film thickness dependencies $G \propto \delta^2$ and $W \propto \delta$ Eq. (71) becomes

$$m = -1 + 2 \left(\frac{\partial \ln Nu}{\partial \ln G} \right)_W + \left(\frac{\partial \ln Nu}{\partial \ln W} \right)_G \tag{72}$$

where the geometric interpretation of the partial derivatives is clear with reference to Fig. 15. Evaluation of these partial derivatives leads to results of the type sketched in Fig. 18, which shows contours of constant m projected on the log W - log G plane† for H = 9. Similar to the case of the log $\mathcal{C}$ - log $\mathcal{R}$ plane discussed in Section 3.3, it is instructive to consider the dependence of m along a straight line of constant $W/\sqrt{G}$ passing through some salient operating point (G, W). Under a contemplated change in the film thickness‡ ($\delta \rightarrow \delta'$) both kinetic parameters

---

* assuming all other quantities (in particular H) remain substantially unchanged. This ceases to be true in the flight regimes where dissociative relaxation in the shock layer becomes important.

† these contours are also included on the isometric drawing of the Nu (G, W; 9) surface shown in Fig. 15.

‡ for a conductivity cell δ may be identified with the volume/active surface ratio. Thus, in considering the effects of a change in δ, one is, in a sense inquiring into the behavior of a "reactor" under a change in surface-to-volume ratio.

$\underline{G}$ and $\underline{W}$ would change but in such a way that the new operating point ($\underline{G}'\underline{W}'$) would lie along this line. If δ' were smaller than δ then $\dot{q}''$ at the new operating point ($\underline{G}'\underline{W}'$) would indeed be larger than at ($\underline{G},\underline{W}$), however the heat flux sensitivity to the contemplated change in δ will be considerably less than proportional to δ^{-1} over an intermediate portion of this line (increasing toward δ^{-1} only for sufficiently small δ). Using Eq. (65), similar statements are seen to be valid for the scale dependence of the steady state surface temperature for radiation cooled leading edge elements.*

Before concluding with a discussion of the effects of surface temperature on the rate of aerodynamic heat input, several comments should be made concerning implicit limitations on the application of the altitude-velocity maps presented in Figs. 11, 12, 13, 16, 17. First, altitude limitations are set by the breakdown of boundary layer theory ($h \approx 250$ Kft. for $R_B \approx 1$ ft.) and the process of shock layer dissociative relaxation (which, in the re-entry vehicle velocity range may be important as low as 200 Kft.; cf. Refs. 58, 59). Second, radiation heat transfer to the surface will begin to contribute significantly ($>$ 10 percent) to the total heat flux in the domain roughly characterized by $\dot{q}'' > 10^3$ BTU/ft.^{2} - sec. (60). Since solid surfaces would have to achieve temperatures of at least 3750°K to re-radiate a heat flux of this magnitude, this justifies neglect of gas cap radiation for most applications involving cooling by radiation alone. Finally, at super-satellite velocities (where cooling solely by radiation is not feasible except at extreme altitudes) ionization phenomena must be accounted for in calculating both the convective and radiative heat flux (61, 62).

3.5 Influence of the Aerodynamic Heat Input Law; Dependence on Surface Temperature Level

A discussion of heat transfer with chemical reaction would not be complete without some mention of the very dramatic effects that can be produced by changes in surface temperature. For example, the input heat flux can have the same value at

*The scale dependence of surface temperature is of interest in the pyrometry of flame gases since extrapolation procedures (to zero diameter) are used to obtain the true flame temperature (6).

three distinct surface temperatures, as pointed out in Ref. 14. As a corollary it should then be possible for three steady state temperatures to exist for a radiation cooled solid in a given environment. This is attributable to the fact that each of the contributions to the total heat flux $\dot{q}'' = \dot{q}''_\lambda + \dot{q}''_D$ has a distinct temperature dependence, and the chemical contribution ($\dot{q}''_D$) can actually increase with increasing surface temperature owing to a strong temperature dependence of the recombination coefficient. Behavior of this type is illustrated in Fig. 19 for the case of stagnation point heat transfer to an axisymetric catalytic solid when the degree of dissociation α_e at the outer edge of the boundary layer is the equilibrium value corresponding to the temperature T_e. As discussed in Section 3.3 this latter condition implies that <u>both</u> $\dot{q}''_\lambda$ and $\dot{q}''_D$ will vanish when the surface reaches the temperature T_e, regardless of its catalytic activity (<u>i.e.</u> for any $\mathcal{C}$). For all surface temperatures lower than T_e the heat flux to a perfect catalyst ($\phi = 1$) is always larger than the heat flux to a completely inactive surface ($\phi = 0$) in the absence of gas phase recombination.* Owing to the choice of ordinate, this difference is represented by the vertical distance $r_D \Delta h_{chem}$, which attains a constant maximum value for surface temperatures below the dissociation "threshhold". The heat flux in the absence of any recombination ($\phi = 0$) increases almost linearly as the surface temperature decreases, as represented by the growth of the vertical distance Δh_f. Now consider the heat flux to a catalyst for which the rate constant k_w increases rapidly with surface temperature (cf. dashed curve, Fig. 19). At low surface temperatures k_w is so small that the heat flux is shown near the nonreactive

---

*Moore and Pallone (<u>63</u>) have provided an exact solution (h = 200 Kft., $M_\infty = 25$, $\mathcal{C} = 0$, $R_B = 1$ ft.) displaying precisely the limiting behavior shown in Fig. 19. For this case T_e ($\approx 6750^\circ K$) is far beyond the destruction temperature of known materials. Interestingly enough, for surface temperatures in the range 2000 - 3000°K, their solution exhibits nonequilibrium properties consistent with the contours presented in Figs. 16 and 17.

value (corresponding to $\phi \approx 0$). At larger temperatures the extent of recombination rises rapidly, possibly attaining a value close to unity for temperatures below T_e. The result is a heat input curve exhibiting two extrema and a region of positive slope on the q''-T_w plane. Following the arguments of Ref. 14, if this were the case a range of intermediate surface temperatures could be statically unstable, depending on the nature of the heat loss-temperature relation. This unstable region would certainly be contained within the two temperatures at which the $\dot{q}''(T_w)$ relation exhibits its extrema, as has been pointed out by Carson (64). Indeed, using the general correlation equation of Ref. 44 Carson has displayed a specific case in which such a region would be expected to exist. This is shown in Fig. 20, applicable to a LiCl surface of nose radius 1.25 ft. coated with lithium chloride, operating at h = 250 Kft., V_∞ = 15 Kft./sec. In this case it can be verified that the non-monotonic behavior occurs for temperatures at which radiation loss alone could not possibly cope with the input heat flux.* But for a radiation cooled solid in a fixed aerodynamic environment two stable steady state surface temperatures are possible only if at some intermediate temperature level

$$\frac{\partial \ln \dot{q}''}{\partial \ln T_w} > n \tag{73}$$

It can be shown from Eqs. (42,43,63) that this is possible only if†

$$\frac{E}{RT_w} > 4n \tag{74}$$

---

*however, radiation loss would be a contributer to whatever heat protection system was adopted.

†Interestingly enough, the recombination rate data used by Carson indicates that this necessary condition would be met at $T_w \approx 540^{\circ}K$ if LiCl were characterized by n = 3.5 or less (cf. Table 1).

where E/R describes the temperature dependence of the rate constant k_w in accord with Eq. (38) and n (= 4 for constant emissivity surfaces) is again given by Eq. (2). Therefore, if over the entire temperature range below the melting point the kinetic parameter E/RT_w never exceeds $4n$, mulitple solutions and hysteresis phenomena (cf. Ref. 14) can be ruled out.* When the exothermic chemical process of interest is surface catalyzed atom recombination, the presence of the factor n (in place of unity) makes this class of phenomena less likely for radiation cooling than for convection cooling. In the latter case it should be remarked that the phenomenon is quite common, in fact Lavrovskaya and Voevodskii (65) have used it to experimentally determine γ and $E/(RT)$ for oxygen and hydrogen recombination on several surfaces.

*unless radiation loss contributes to another loss mechanism which becomes less effective at higher surface temperatures.

4. CONCLUDING REMARKS

In parts 2 and 3 we have emphasized aspects of radiation cooling which have received relatively little attention but which may in practice play a very important role in determining steady state surface temperatures. While the treatment has been simplified so as to illustrate the major effects in most particular cases more refined computational methods can be brought to bear to increase accuracy.* But, particularly in the area of chemical nonequilibrium effects, where accurate computations may be very time-consuming (and, hence, expensive), an overall picture of the regimes in which large effects are possible is of interest so that the heavy artillery can at least be trained on the proper targets.

The analysis also displays the important similitude parameters and input data requirements. In the area of materials properties it is clear that in order to make accurate surface temperature predictions high temperature data is urgently needed on (i) emissivity, (ii) thermal conductivity, (iii) recombination coefficients. Long extrapolations which are not guided by sound theory can prove quite inaccurate in each of these categories. To illustrate this in case (iii) we have only to look at existing recombination rate data on quartz surfaces (66,67), where marked deviations from simple Arrhenius behavior is evident. For nitrogen atoms on quartz at temperatures near 1200°K (67) the rate constant k_w appears to obey a relation of the form of Eq. (38) but with $A \propto T^{-\frac{1}{2}}$. This implies the existence of a temperature at which γ would maximize; a phenomenon potentially important for high temperature ceramic materials.†

---

* An obvious improvement would result, for instance, from use of enthalpy instead of temperature as the dependent variable in the convection part of the problem.

† For nitrogen atoms on quartz (800°-1200°K) data (67) indicate that γ would attain a maximum value somewhat less than 2.5×10^{-3} at an extrapolated temperature of 2300°K (which is well above its melting point).

In the area of gas phase properties the demands are of course those already familiar in aerodynamic heating calculations; i.e. better information on transport properties (of multicomponent gases) and chemical kinetic constants,* particularly at high temperatures. Here even interpolation is hazardous, as illustrated by the intriguing result (48) that the temperature dependent cross sections for the $H-H_2$ interaction are probably not intermediate between those of H-H and H_2-H_2.

Finally, mention should be made of problem areas in transport theory implicitly or explicitly suggested by earlier examples. These would include generalized predictions of the effects (on surface temperature) of (i) mutual radiation transfer, as encountered in external flow over locally concave bodies or for internal flows (ii) finite material thermal conductivity [cf. Sections 2.2 and Ref. 68] and finite thermal diffusivity (for analyses of transient behavior) (iii) simultaneous mass transfer, e.g. as encountered in using charring ablators (iv) piecewise discontinuous emissivity [cf. Section 2.3] (v) departures from continuum gas dynamic behavior at high altitudes (vi) homogeneous and heterogeneous chemical kinetic phenomena [cf. Sections 3.2-3.5] and (vii) aerothermoelastic coupling phenomena (69).

ACKNOWLEDGEMENT

The financial support of the Propulsion Division, Office of Aerospace Research, Air Force Office of Scientific Research is gratefully acknowledged. It is also a pleasure to thank C. Spofford and F. Kuehner for their computational assistance in preparing Parts 2 and 3 respectively.

---

* the result that aerodynamic heat flux is approximately dependent only on enthalpy difference (across the boundary layer) has led, with distressing frequency, to the erroneous impression that chemical kinetics do not exert a strong influence on heat transfer. The fact is that chemical reaction rates play a major role in establishing the magnitude of Δh in most hypersonic applications. Fig. 17 indicates that local heat fluxes can easily vary by a factor of 5, depending upon the extent of recombination.

REFERENCES

1 Fay, J. A. and Riddell, F. R., J. Aeronaut. Sci. 25, 1958, 73.

2 Lees, L, Combustion and Propulsion, Third Agard Colloquium, New York, Pergamon Press, 1959, 451-499.

3 Rosner, D. E., Jet Propulsion, 28, No. 7, 1958, 445-451.

4 Rosner, D. E., ARS Journal, 31, 1961, 1013-1015, ibid. 31, 1961, 1469.

5 Robbins, W. H. and Todd, C. A., NASA TN D-878, 1962.

6 Gaydon, A. G. and Wolfhard, H. G., Flames, Their Structure and Radiation, Chapman Hall, Second Ed., London, 1960, 277.

7 Rosner, D. E., ARS Journal, 32, No. 7, 1962, 1065-1073.

8 Rosner, D. E., Trans. of the ASME, Series C, J. of Heat Trans., 84, No. 4, 1962, 386-394.

9 Lighthill, M. J., Proc. Roy. Soc., London, Ser. A, 202, 1950, 359-377.

10 Rosner, D. E., AeroChem TM-18, AFOSR TN 60-331, 1959.

11 Naysmith, A. and Woodley, J. G., RAE Technical Note AERO 2807, 1962.

12 Czysz, P. and Smith, R. R., ASD TDR 62-71, ASTIA AD-275 373, 1962.

13 Wing, L. D., Space/Aeronautics, 34, No. 4, 1960, 187-196.

14 Rosner, D. E., Jet Propulsion, 28, 1958, 402-403.

15 Rosner, D. E., AeroChem TP-54, 1962.

16 Spalding, D. B., ASME, International Heat Transfer Conference, Paper No. 15, 1961, 439-446.

17 Curle, N., Aeronaut. Res. Council, Great Britain, ARC 20, ASTIA AD-220 213, 1958, 482.

18 Rosner, D. E., AeroChem TP-35, AIChE Preprint No. 135, AIChE J.(in press) 1961.

19 Rosner, D. E., AeroChem TP-50, (submitted to Chem. Egn. Sci.), 1962.

20 Fishenden, M., Int. J. Heat Mass Transfer, 5, 1962, 67-76.

21 Opik, E. J., Physics of Meteor Flight in the Atmosphere, Interscience Publishers, Inc., New York, 1958.

22 Strong, J., Procedures in Experimental Physics, Prentice Hall, N. J., 1938, 509.

23 Rosner, D. E., Jet Propulsion, 28, No. 8, Part 1, 1958, 555.

24 Ambrok, G. S., Soviet Physics, Tech. Physics, 2, No. 7, 1957, 1979-1986.

25 Acrivos, A., Chem. Engr. Sci., 17, 1962, 457-465.

26 Chambers, R. L. and Somers, E. V., J. Heat Transfer, Trans. ASME, Series C, 81, 1959, 327-329.

27 Rosner, D. E., J. Aero/Space Sci., 26, 1959, 281-286.

28 Rosner, D. E., AeroChem TP-14, AFOSR TN 60-887, 1959.

29 Brant, J. A., Eckert, E. R. G. and Irvine, T. E., Jr., Proc. 1960 Heat Transfer and Fluid Mechanics Institute, Stanford University Press, 1960, 220-228.

30 Rosner, D. E., AeroChem TP (in preparation).

31 Polhausen, E., Z. angew. Math. Mech., 1, 1921, 115-121.

32 Chapman, D. R. and Rubesin, J. Aeronaut. Sci., 16, 1949, 547.

33 Eckert, E. R. G, WADC Tech. Rpt. April 1954, 54-70.

34 Eckert, E. R. G., WADC Tech. Report, 1960, 59-624.

35 Mayer, E., ARS Journal, 31, No. 7, 1961, 911-917.

36 Chung, P. M., Liu, S. W. and Mirels, H., Aerospace Rpt. TDR-69, TN-1, 1962.

37 Vaulin, E. P., Soviet Physics, 2, No. 2, 1957, 187-191.

38 Rosner, D. E., J. Aero/Space Sci., 26, 1959, 384-385.

39 Rosner, D. E., PhD Dissertation, Princeton University, Aeronaut. Egnr. Dept., 1960.

40 Rosner, D. E., ARL 99 Part 1, 1961, AeroChem TP-22, 1961.

41 Frank-Kamenetskii, D. A., Diffusion and Heat Exchange in Chemical Kinetics, Princeton University Press, Princeton, N. J., 1955.

42 Scala, S. M., Proc. 3rd U. S. National Congress of Applied Mechanics, ASME, 1958, 799-806.

43 Goulard, R. J., Jet Propulsion, 28, 1958, 737-745.

44 Rosner, D. E., ARS Journal, 29, 1959, 215-216.

45 Inger, G. R., Douglas Aircraft Co., Rpt. SM-38936, 1962.

46 Gibson, W., IAS Paper 63-70; Presented at the IAS 31st Annual Meeting, N. Y.,1963.

47 Hall, J. G., Eschenroeder, A. Q. and Marrone, P. V., Cornell Aero Lab. Rpt. No. AF-1413-A-2, Buffalo, N. Y., 1962.

48 Vanderslice, J. T., Weissman, S., Mason, E. A. and Fallon, R. J., Physics of Fluids, 5, No. 2, 1962, 155-164.

49 Detra, R. W. and Hidalgo, H., ARS Journal, 31, No. 3, 1961, 318.

50 Huber, P. W., NACA TN-4352, 1958.

51 Masson, D. J. and Gaxely, C., Aeronaut. Engr. Review, 15, 1956.

52 Whalen, R. J., J. Aerospace Sci., 29, No. 10, 1962, 1222-1237.

53 Broadwell, J. E., J. Fluid Mech., 4, Pt. 2, 1958.

54 Chung, P. M., NASA TN D-306, 1960.

55 Clark, J. F., J. Fluid Mech., 4, Pt. 5, 1958, 441-465.

56 Inger, G. R., ARS Journal, 32, No. 11, 1962, 1743-1744.

57 Grier, N. T. and Sands, N., NASA Technical Note D-8665, 1961.

58 Chung, P. M., NASA Technical Rpt. R-109, 1961.

59 Gibson, W. E., ARS Journal, 32, No. 2, 1962, 285-287.

60 Kivel, B., J. Aero/Space Sci., 28, No. 2, 1961, 96-101.

61 Scala, S. M., ASD Tech. Rpt. 61-645, 1961, 530-592.

62 Fay, J. A. and Kemp, N. H., IAS Paper No. 63-60; Presented at the IAS 31st Annual Meeting, New York, N. Y., 1963.

63 Moore, J. A. and Pallone, A., AVCO Corp. Res. and Adv. Dev. Div., Tech. Memo No. RAD-TM-62-59, 1962.

64 Carson, B. H., MSE Thesis, Dept. of Aeronaut. Engr., Pennsylvania State University, 1961.

65 Lavrovskaya, G. K. and Voevodskii, V. V., Zhur. Fiz. Khim. 25, 1050-1058, 1951.

66 Greaves, J. C. and Linnett, J. W. Trans. Faraday Society, 55, No. 440, 1959, 1338-1361.

67 Marshall, T., J. Chem. Phys., 37, No. 10, 1962, 2501-2502.

68 Abarbanel, S., J. Aerospace Science, 28, No. 4, 1961, 299-307.

69 Brull, M. A., Paper presented at the GE-AFOSR Symposium on Manned Lifting Planetary Entry, Philadelphia, October 29-31, 1962.

NOMENCLATURE

A	pre-exponential factor in Arrhenius expression; Eq. (38)
C	nondimensional catalysis parameter, Eq. (27)
$\bar{c}_p$	specific heat of mixture (frozen)
D_{12}	atom-molecule binary diffusion coefficient
E	activation energy; Eq. (38)
G	$(\delta^2/D_{12})/C$; gas phase recombination rate parameter
H	$r_D \cdot \Delta h_{chem,\ eq}/\Delta h_f$
h	enthalpy of gas mixture
h	altitude
k	Boltzmann constant
k_w	first order rate constant for heterogeneous recombination
Le	Lewis number $\equiv D_{12}/[\lambda/(\rho c_p)]$
L	total length along surface
m	exponent defined by Eq. (66)
m_1	atomic mass
M_∞	Mach number
Nu	Nusselt number
n	true reaction order, Eq. (5); or exponent defined by Eq. (2)
n_1	atom number density
p	total pressure
Pr_λ	Prandtl number for heat conduction $= (\mu/\rho)/[\lambda/(\rho c_p)]$
Pr_D	Prandtl number for diffusion $= (\mu/\rho)/D_{12}$
$\dot{q}''$	heat flux input at surface
Q	heat of recombination
r_v	recovery factor for free stream kinetic energy; Eq. (31)
r_D	recovery factor for chemical energy; Eq. (33)

R_B	nose radius of body
$\bar{R}$	universal gas constant
$\mathcal{R}$	nondimensional convection-radiation parameter; Eq. (14)
$\dot{R}'''$	local rate of reaction
$\bar{St}$	Stanton number
t	wall thickness
$\bar{T}$	absolute temperature
$\bar{T}^o$	total temperature defined by Eqs. (29,32,45)
$\bar{T}_\varepsilon$	characteristic convection-radiation temperature; Eq. (57)
u	component of local gas velocity parallel to surface element
V_∞	velocity of vehicle relative to undisturbed atmosphere
W	catalytic parameter defined by Eq. (70)
x	distance along solid surface
y	distance normal to solid surface
z	nondimensional coordinate defined by Eq. (15), cf. Table 2
α	local mass fraction of reactant (atoms)
β	inviscid velocity gradient at nose; cf. Fig. 19
γ	recombination coefficient; Eq. (60)
δ	plate spacing, or boundary layer thickness
ε_w	total hemispheric emissivity of surface
ζ	dummy variable
η	normalized local reaction rate or radiative transfer rate; cf. Table 2
$\bar{\eta}$	catalyst or radiation effectiveness factor; cf. Table 2
$\partial\bar{T}$	local driving force for diffusion or heat transfer
θ	normalized local surface temperature
θ_*	discriminant defined by Eq. (51)
λ	thermal conductivity of mixture (frozen)
λ'	thermal conductivity of solid

μ	dynamic viscosity of mixture
ν	kinematic viscosity of mixture
ρ	absolute density of mixture
σ	Stefan-Boltzmann radiation constant
τ	recombination relaxation time (54) in gas phase
$\bar{\tau}$	θ/θ_*; Eq. (56)
ϕ	extent of recombination; Eq. (47)
ϕ	local transfer rate coefficient; cf. Table 2
$\bar{\phi}$	global transfer rate coefficient; cf. Table 2
ψ	Von Mises stream function
ω	parameter; = 2 for laminar boundary layer flow; = 5 for turbulent boundary layer flow

Subscripts

chem	chemical contribution
D	pertaining to diffusion
e	at outer edge of boundary layer
eq	pertaining to local thermochemical equilibrium
f	chemically frozen
G	at constant G
I	inert
iso	isothermal
max	maximum
min	minimum
r	pertaining to recovery condition; Eqs. (31)
s	behind shock
w	at the wall (gas/solid interface)
W	at constant W

λ	pertaining to molecular conduction
1	atoms
2	molecules
∞	at upstream infinity

Operators

Δ	change in
ln	natural logarithm
O( )	order of magnitude of

LIST OF FIGURES

LIST OF FIGURES (continued)

LIST OF TABLES

TABLE I

APPROXIMATE TEMPERATURE DEPENDENCE OF TOTAL RADIATION FLUX FROM HEATED SOLID SURFACES

Surface	Temperature Range (^{o}K)	n	Ref.
opaque quartz (vitreosil)	530-1090	3.5	20
alumina ceramic	530-1090	2.5	20
thoria ceramic	530-1090	2.3	20
magnesia ceramic	530-1090	2.5	20
quartz glass (2 mm)	530-1090	2.9	20
iron (micrometeor)	1500-3000	4.65	21
iron	700-1300	5.55	22
nichrome	325-1310	4.1	22
polished tungsten	420-530	5.4	20
polished magnesium	420-530	5.1	20
molybdenum	420-530	5.2	20
98% pure polished aluminum[a]	420-530	5.4	20
nickel	463-1280	4.65	22
pure polished silver	420-530	4.0	20
silver	610-980	4.1	22
pure polished platinum	420-530	4.9	20
platinum	640-1150	5.0	22

[a] Ref. 20 also cites data for aluminum which suggests $n \approx 4.9$ in this same temperature range.

TABLE 2

ANALOGY BETWEEN SURFACE CATALYSIS AND RADIATION COOLING FOR THE FLOW OF A SLIGHTLY VISCOUS FLUID OVER A FLAT PLATE

Quantity	Surface Catalysis	Radiation Cooling
Unknown	$\alpha = \alpha_w / \alpha_e$	$\theta = T_w / T_e$
Independent Variable	$z = C \cdot (x/L)^{\frac{1}{\omega}}$	$z = \mathcal{R} \cdot (x/L)^{\frac{1}{\omega}}$
Parameters	n = reaction order	$n = 4 + d(\ln \varepsilon_w)/d(\ln T)$
	$C = \dfrac{k_w \cdot (\rho \alpha_e)^n}{Nu_{D,iso}(L) D \rho \alpha_e / L}$	$\mathcal{R} = \dfrac{\varepsilon_w(T_e) \cdot \sigma T_e^4}{Nu_{\lambda,iso}(L) \lambda T_e / L}$
Local Coefficients	$\eta = \dfrac{\text{Actual Local Rate}}{k (\rho \alpha_e)^n}$	$\eta = \dfrac{\text{Actual Local Rate}}{\varepsilon_w(T_e) \cdot \sigma T_e^4}$
	$\phi = \dfrac{\text{Actual Local Rate}}{\text{Convective Rate } \alpha_w \to 0}$	$\phi = \dfrac{\text{Actual Local Rate}}{\text{Convective Rate, } T_w \to 0}$
Integrated Coefficients	$\bar{\eta} = \dfrac{\text{Actual Over-all Rate}}{k (\rho \alpha_e)^n L}$	$\bar{\eta} = \dfrac{\text{Actual Over-all Rate}}{\varepsilon_w(T_e) \cdot \sigma T_e^4 L}$
Integrated Coefficients	$\bar{\phi} = \dfrac{\text{Actual Over-all Rate}}{\text{Convective Rate}, \alpha_w \to 0}$	$\bar{\phi} = \dfrac{\text{Actual Over-all Rate}}{\text{Convective Rate, } T_w \to 0}$

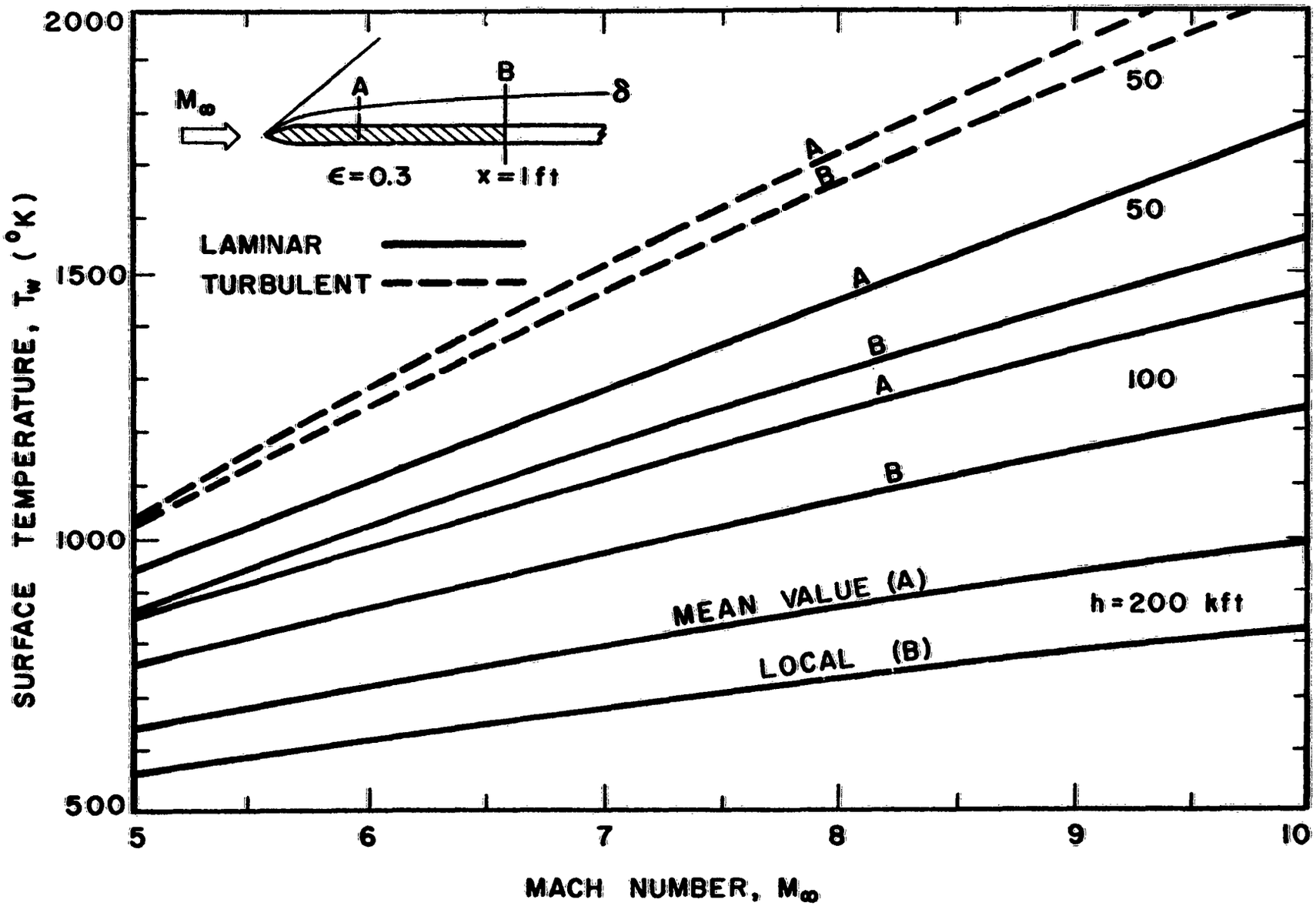

Fig. 1 Steady state surface temperatures for radiating flat plates in air (after Naysmith and Woodley)

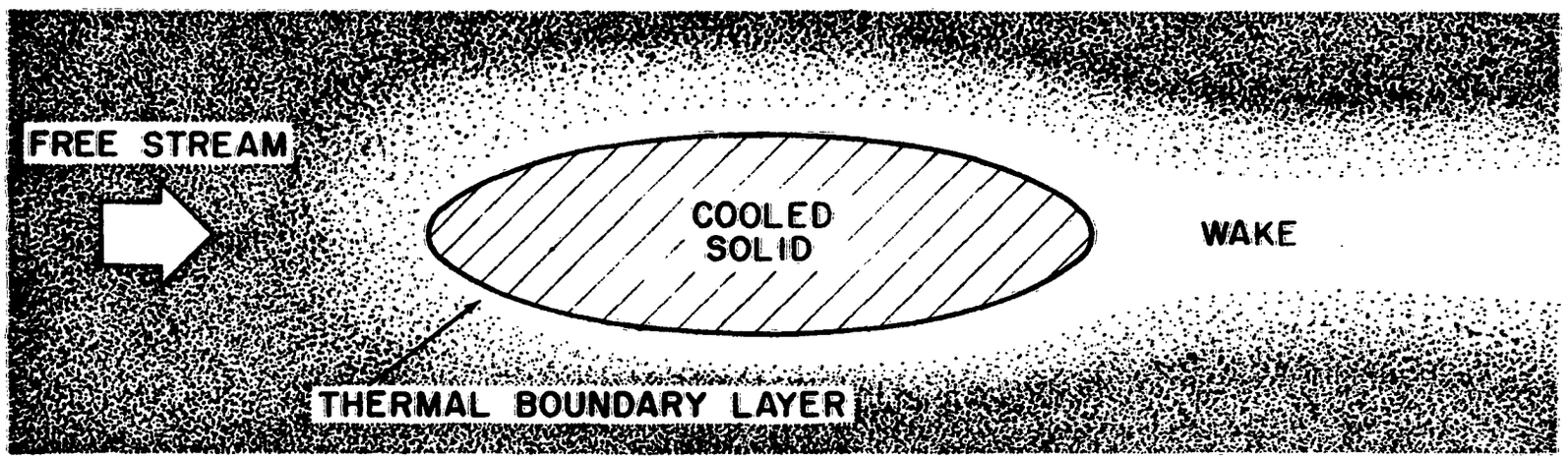

CONVECTIVE HEAT TRANSFER, $\frac{UL}{\alpha} >> 1$

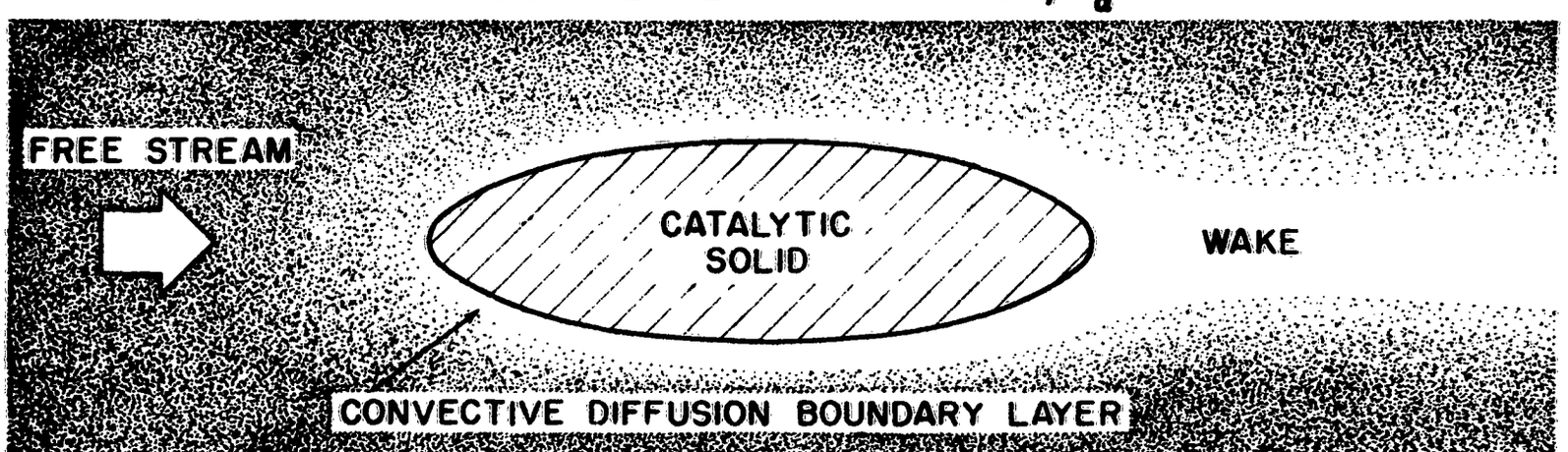

CONVECTIVE MATERIAL TRANSFER, $\frac{UL}{D} >> 1$

Fig. 2 Analogy between radiation cooling and chemical surface catalysis in flow systems

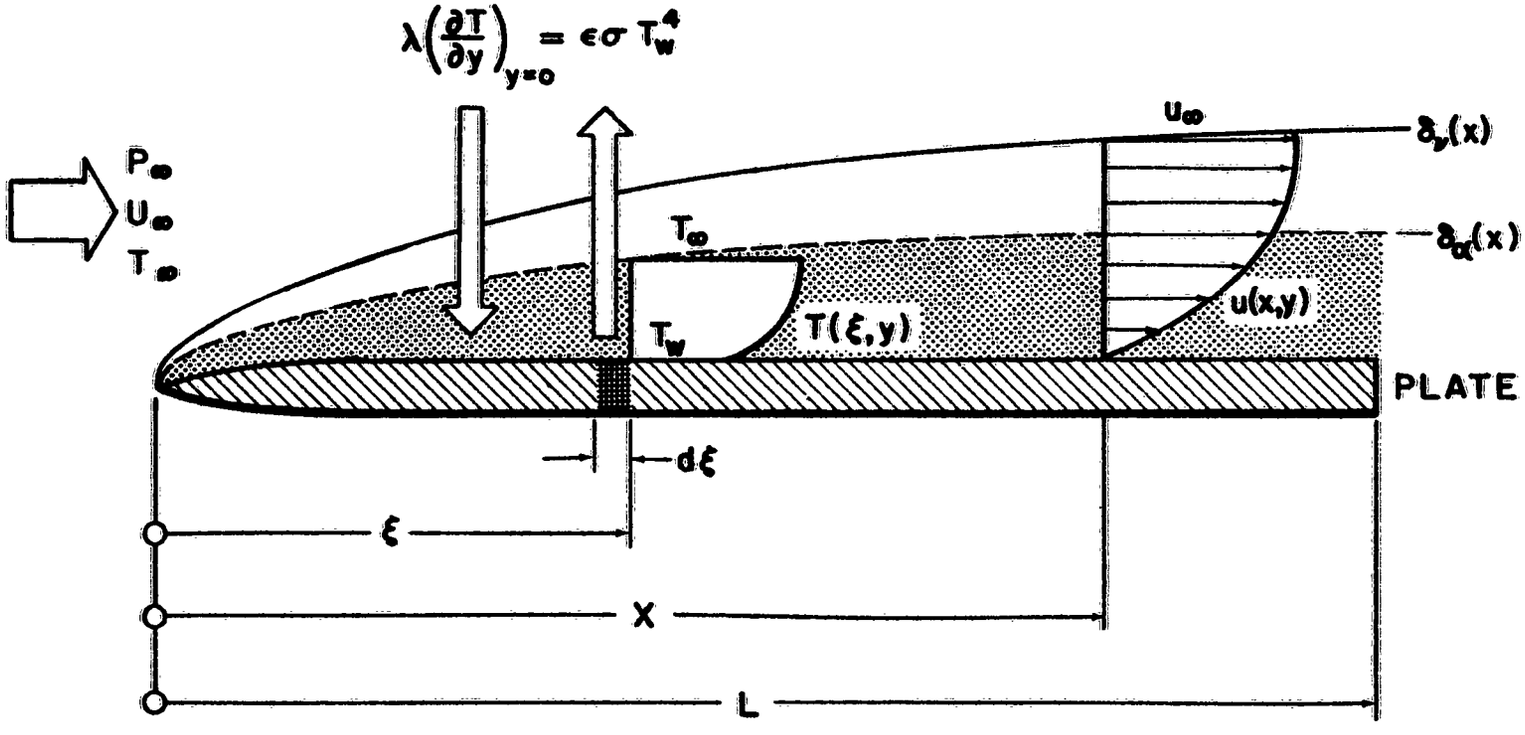

Fig. 3 Geometry and nomenclature; radiation cooled flat plate

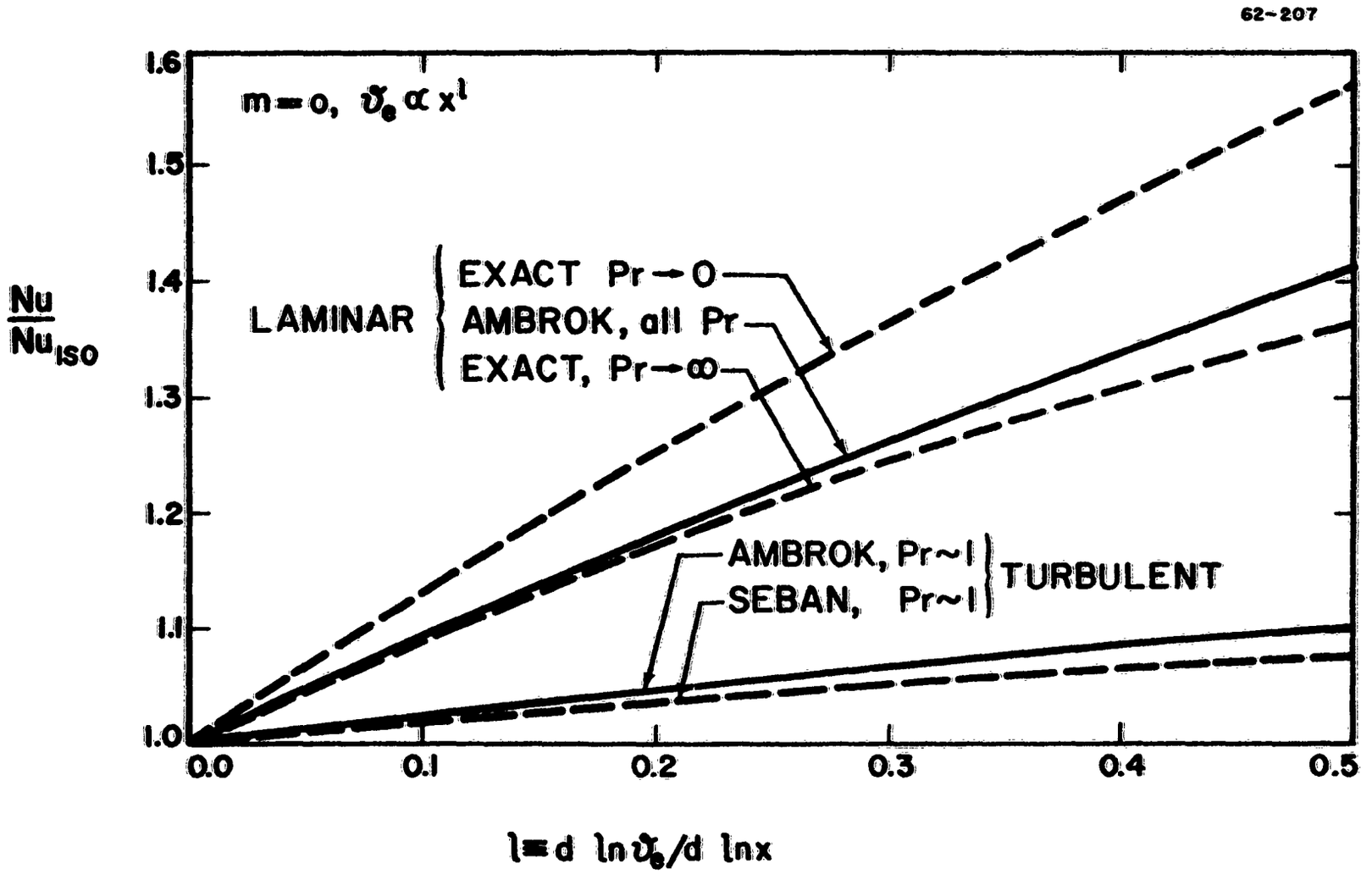

Fig. 4 Effect of a nonisothermal surface on the magnitude of the local heat transfer coefficient; boundary layer flow over a flat plate

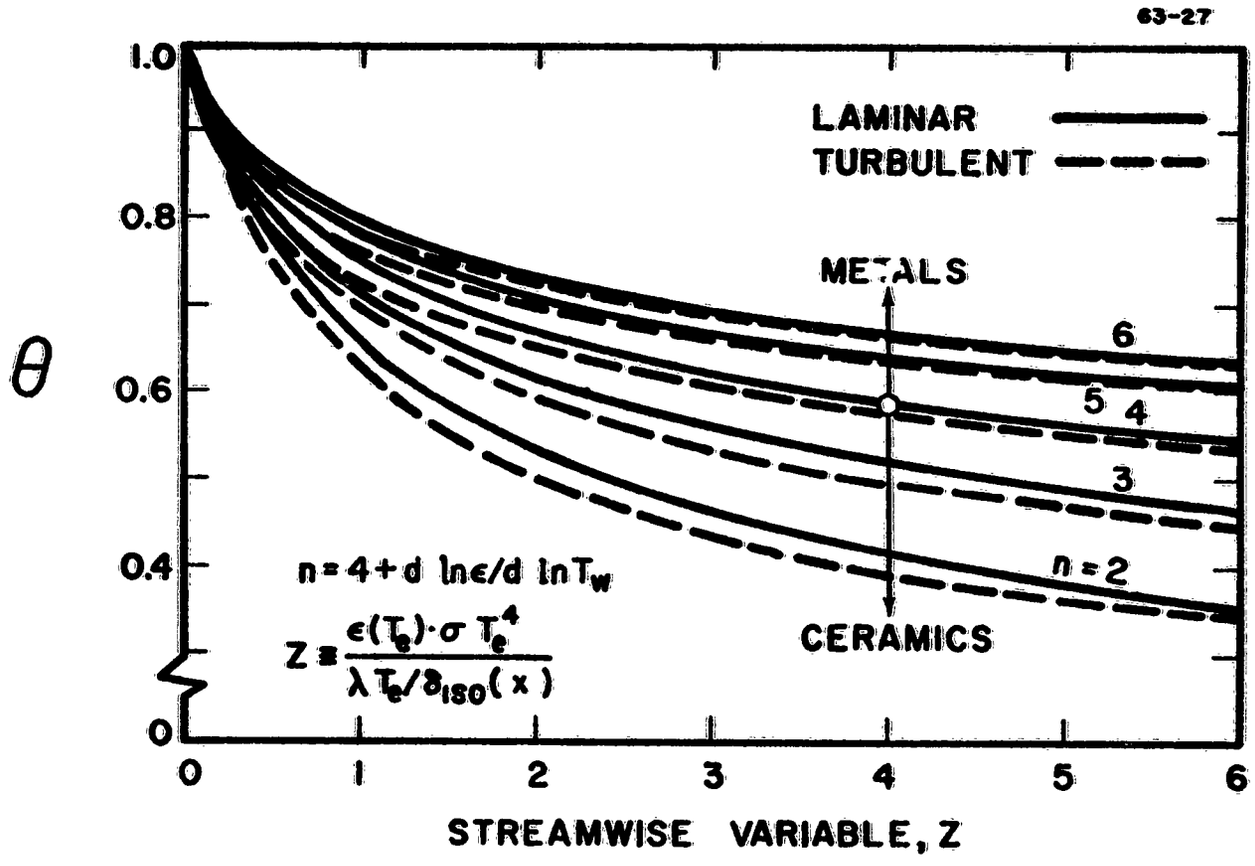

Fig. 5 Steady-state surface temperature distribution for radiation cooled flat plates with power-law emissivity-temperature relation

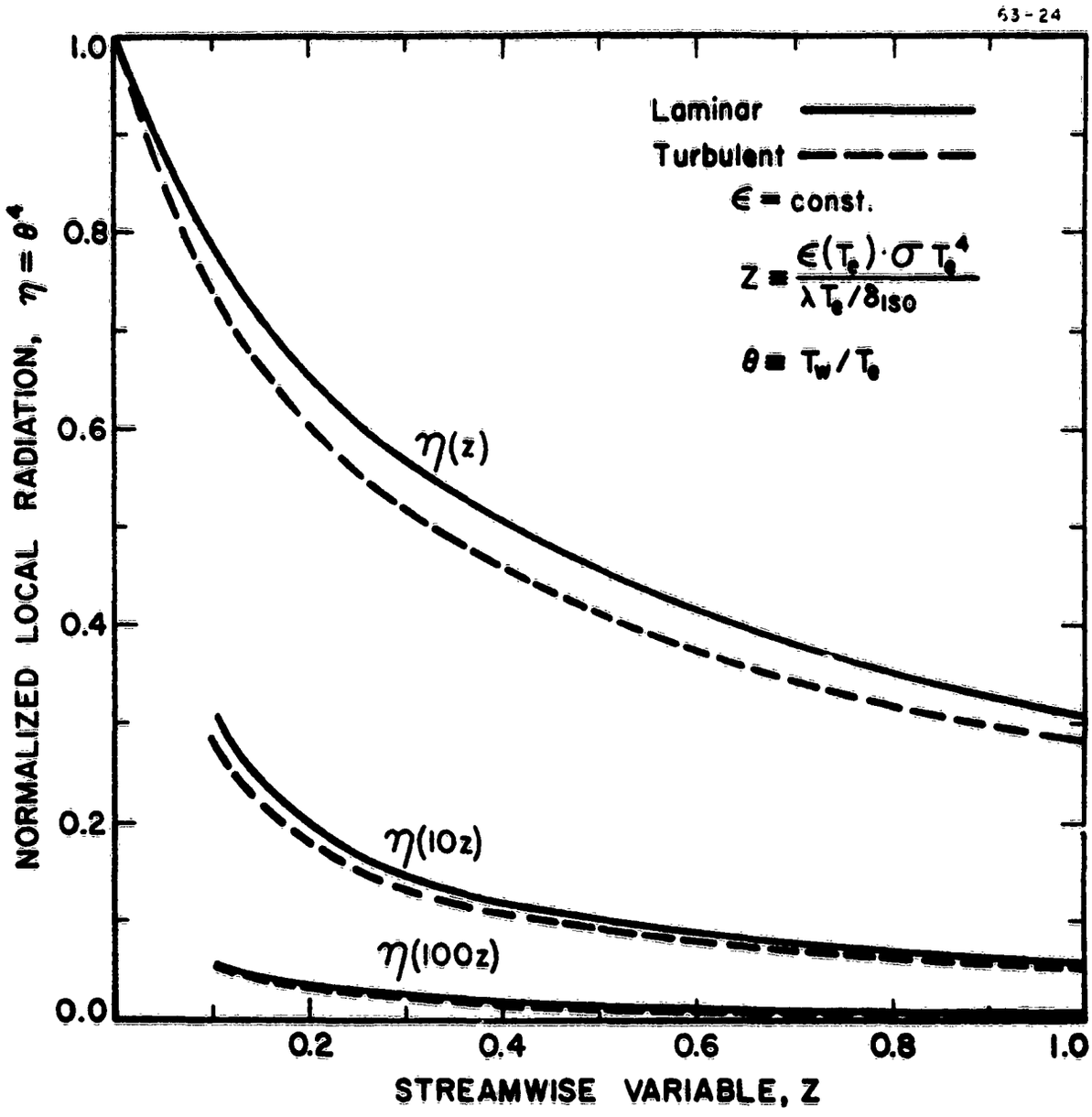

Fig. 6 Normalized distribution of radiative flux for constant emissivity flat plates

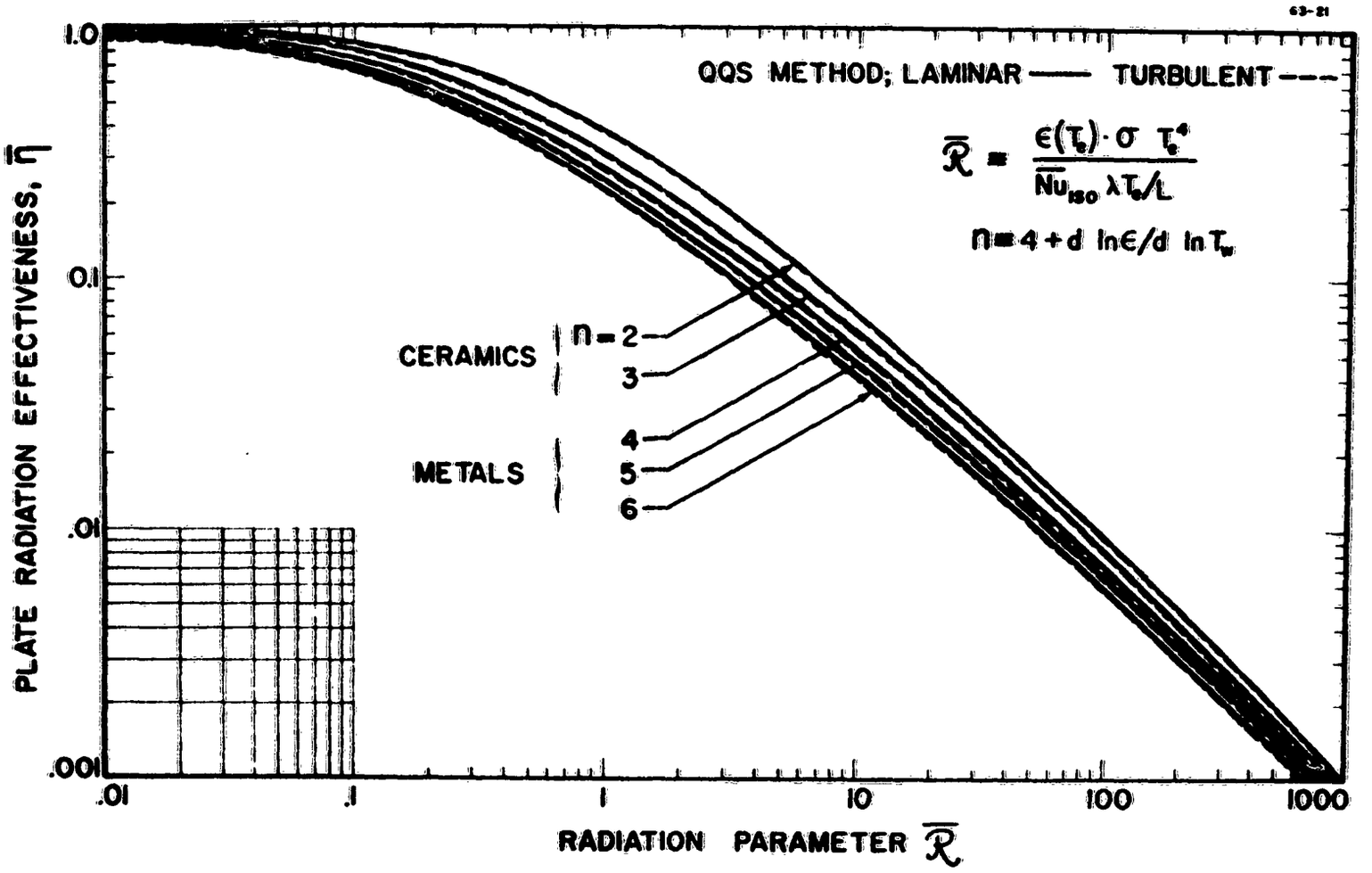

Fig. 7 Integrated radiation effectiveness factors for flat plates with power-law emissivity-temperature relation

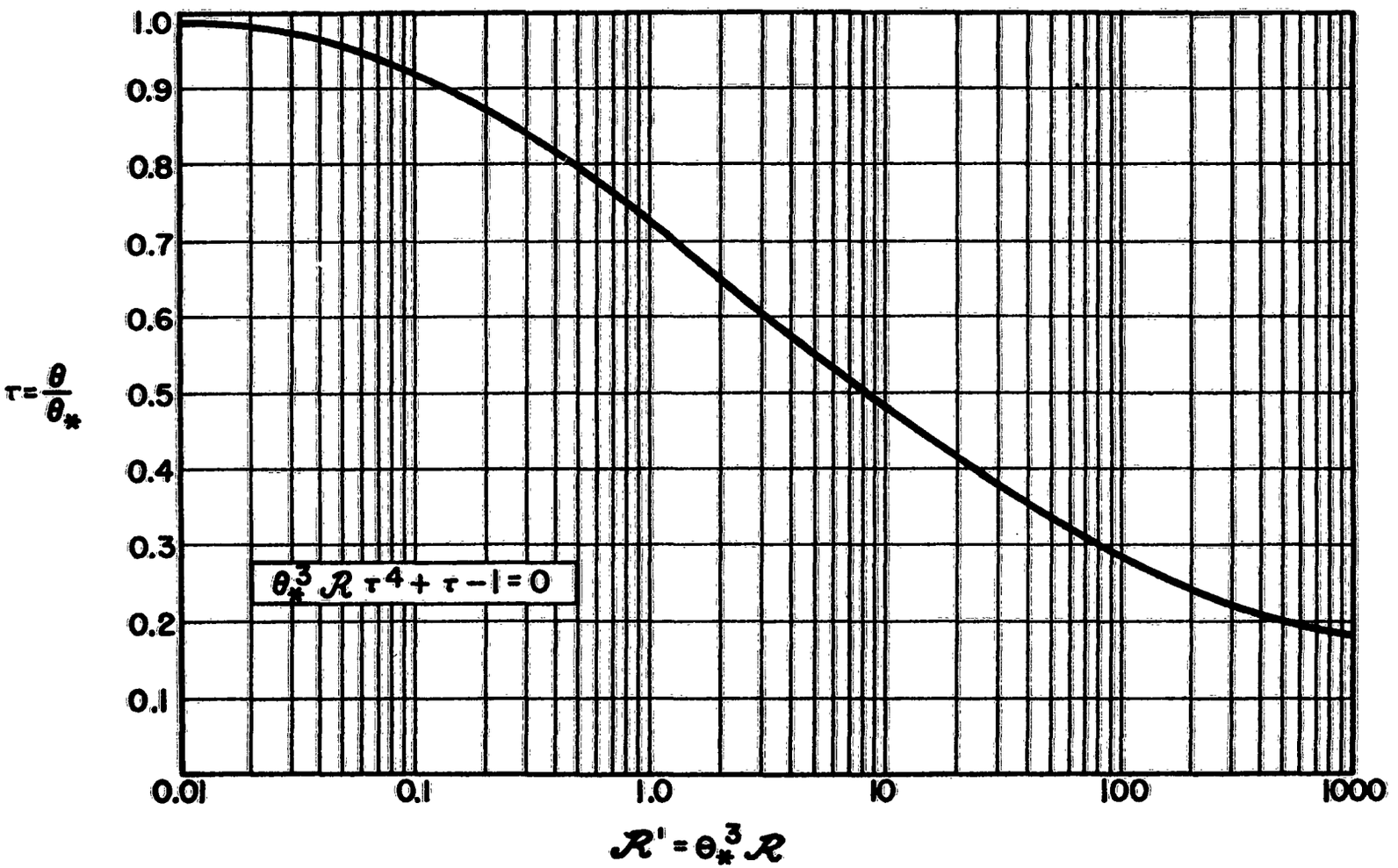

Fig. 8 Graphical solution of the basic quartic equation of radiation cooling theory

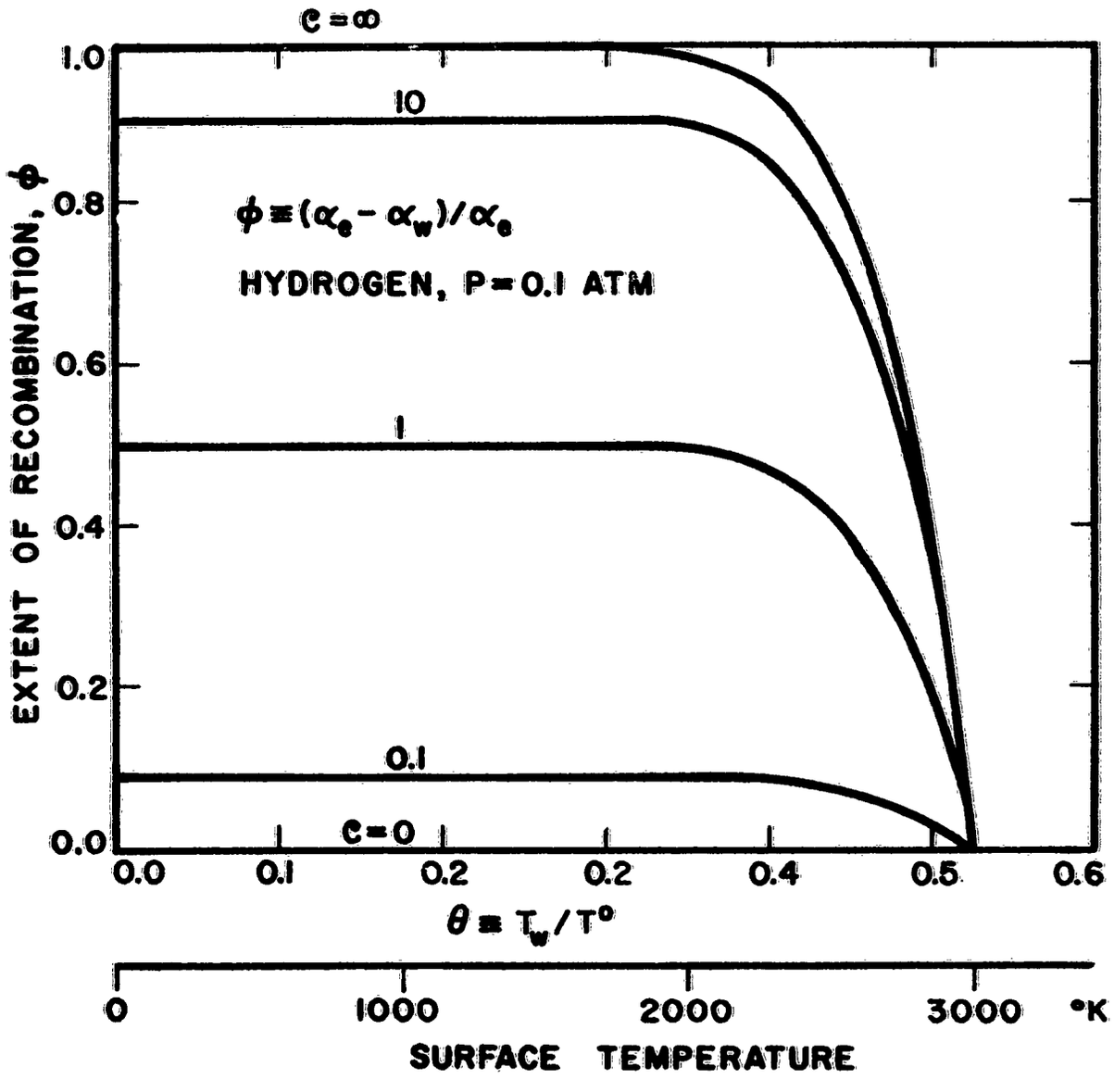

Fig. 9 Dependence of the extent of recombination on surface temperature for catalytic solids of arbitrary activity in hydrogen ($p = 0.1$ atm, $T_e = 3000^oK$)

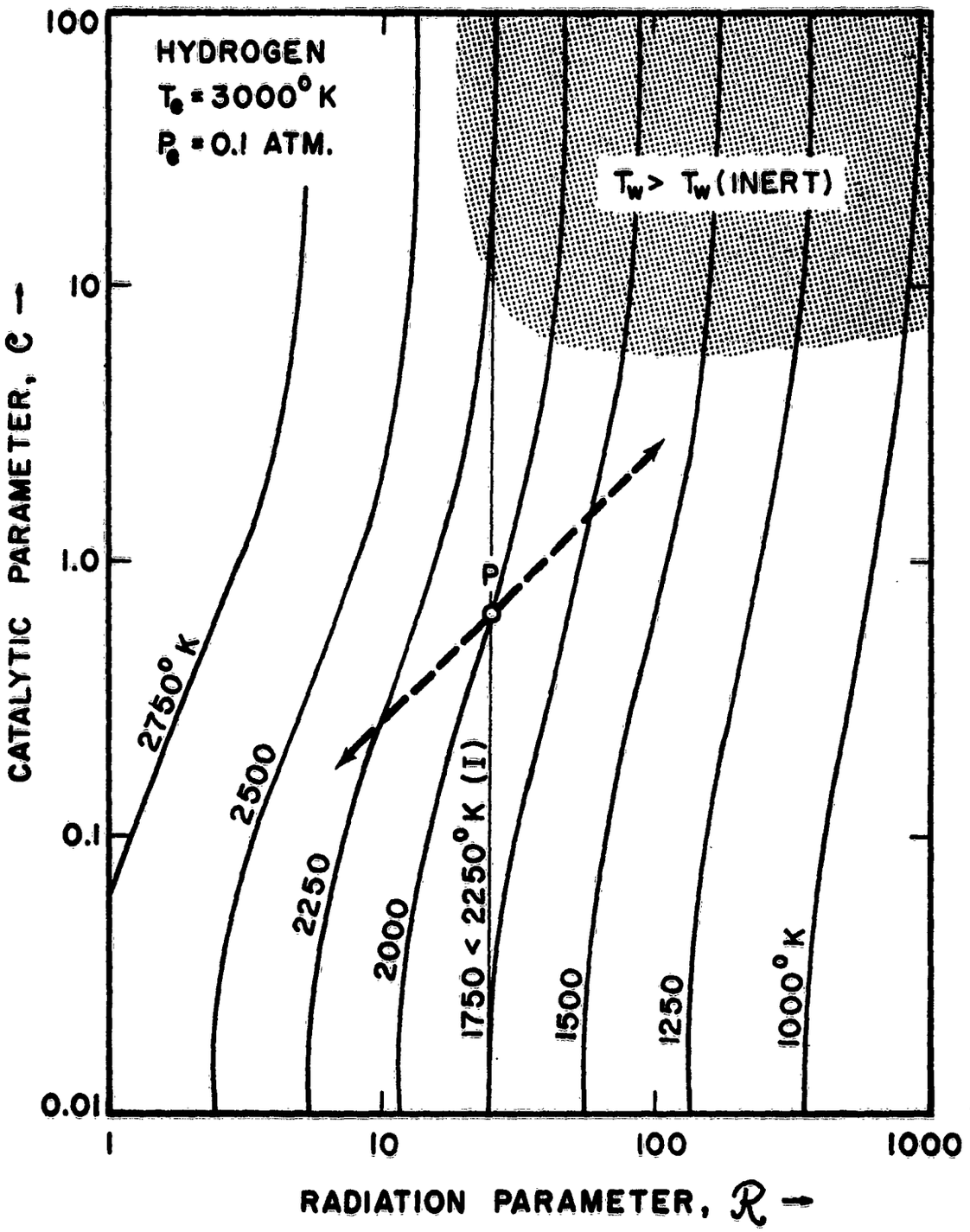

Fig. 10 Locii of constant surface temperature for radiation cooled catalysts of arbitrary activity in hydrogen (p = 0.1 atm, T_e = 3000°K)

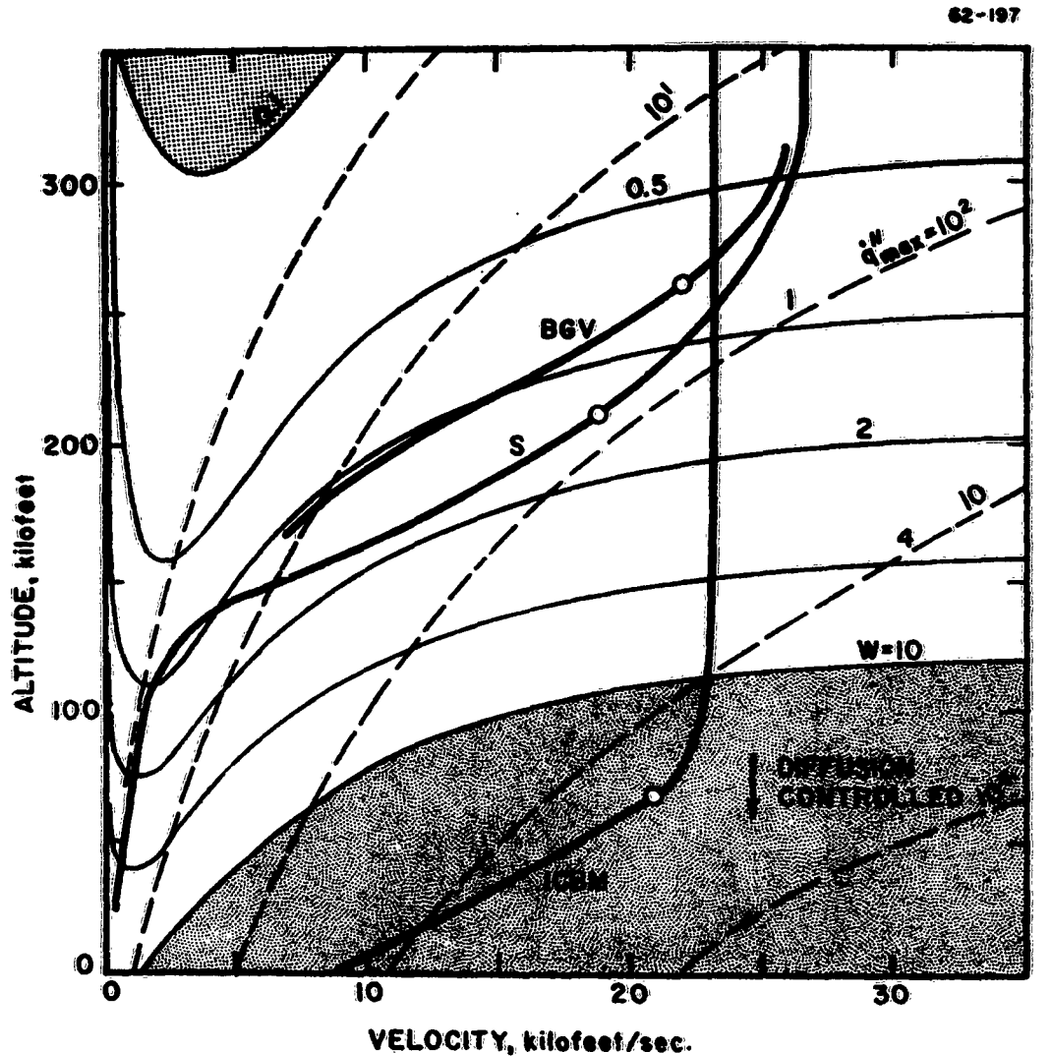

Fig. // Contour map of the catalytic parameter W on the altitude - velocity plane (R_B = 1 ft; T_w = 700°K, $\gamma = 10^{-2}$)

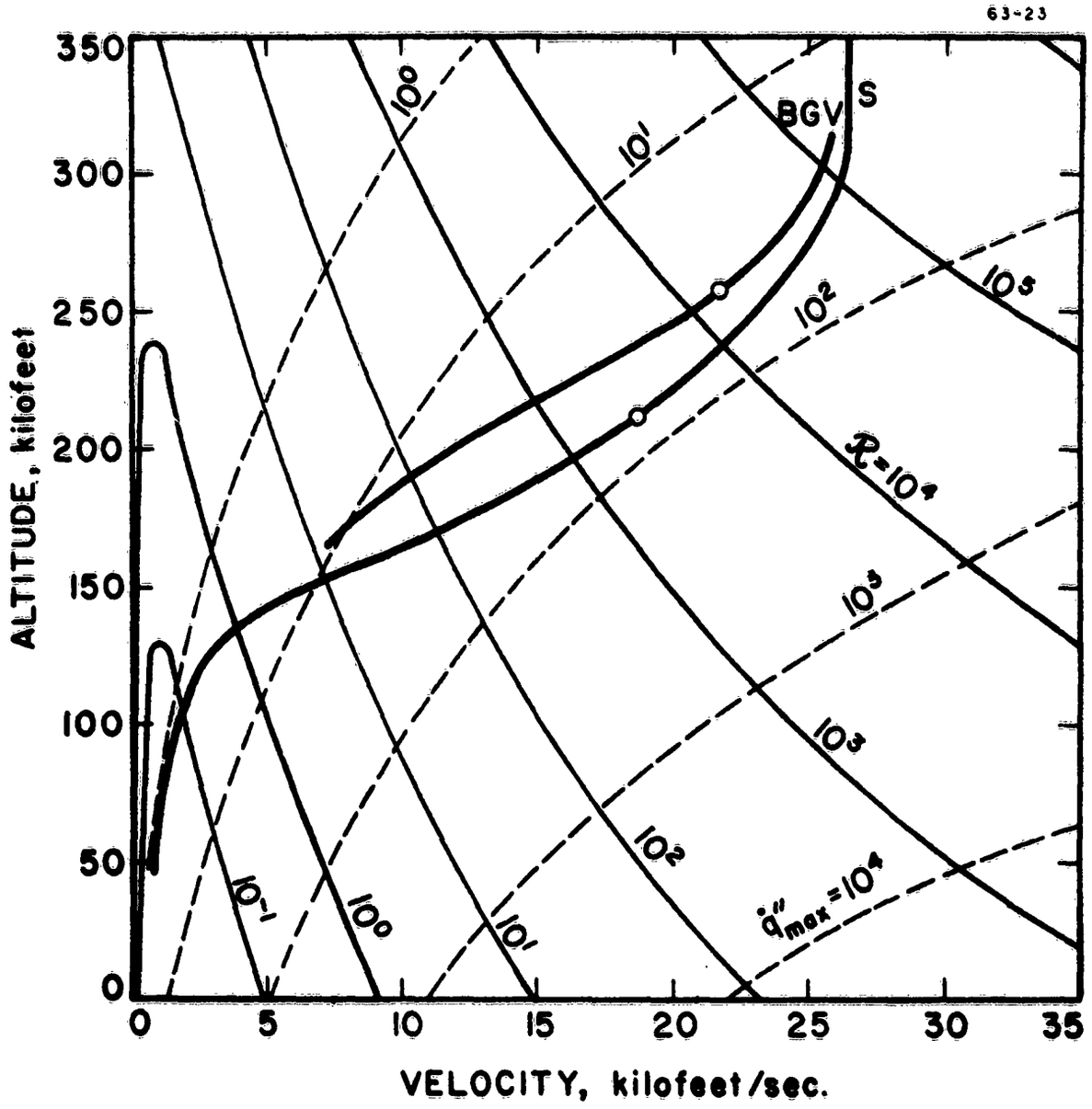

Fig. 12 Contour map of the radiation parameter $\mathcal{R}$ on the altitude-velocity plane (R_B = 1 ft, ϵ = 0.5)

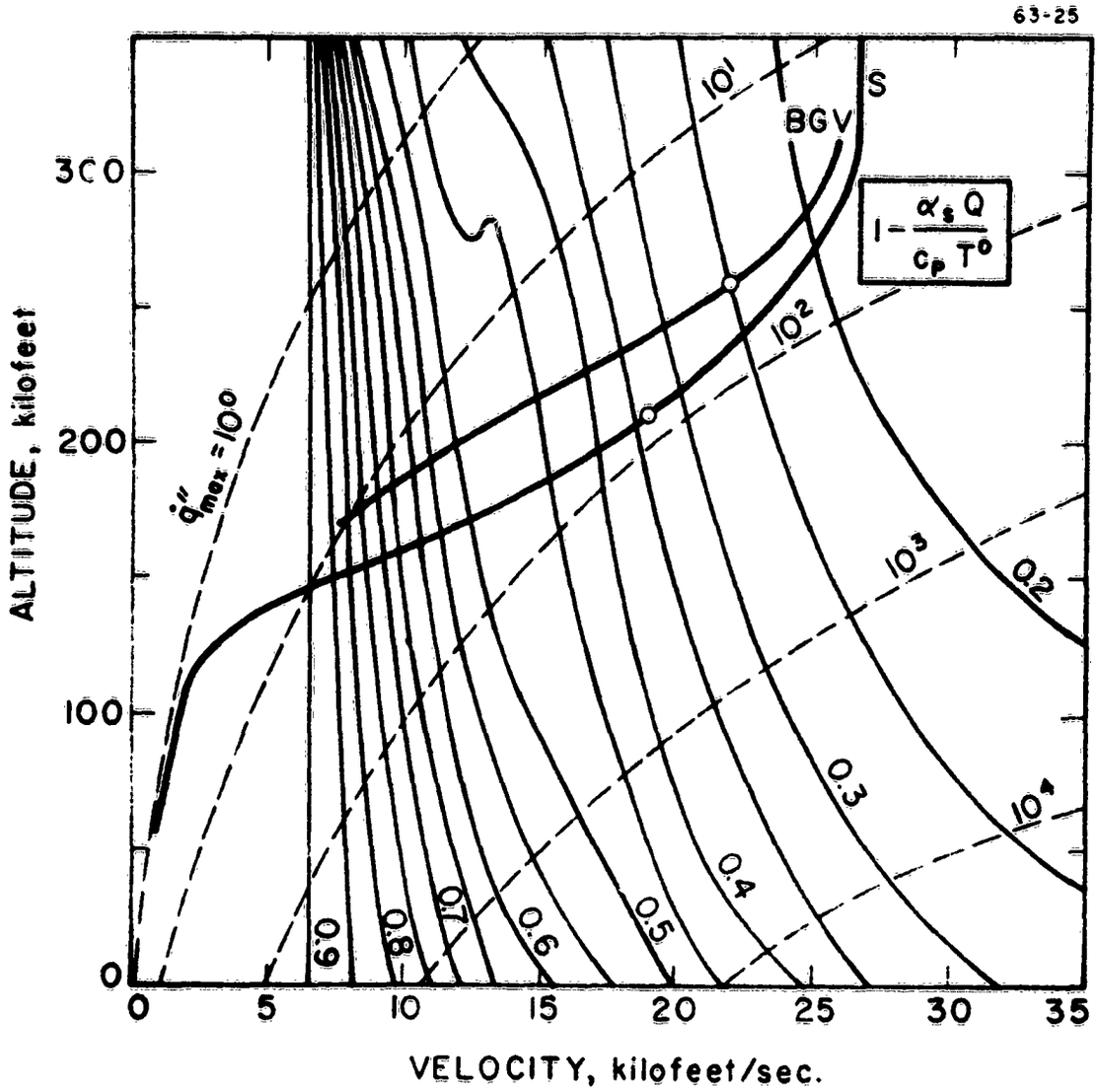

Fig. 13 Qualitative behavior of $\theta_{*,min}$ on the altitude-velocity plane

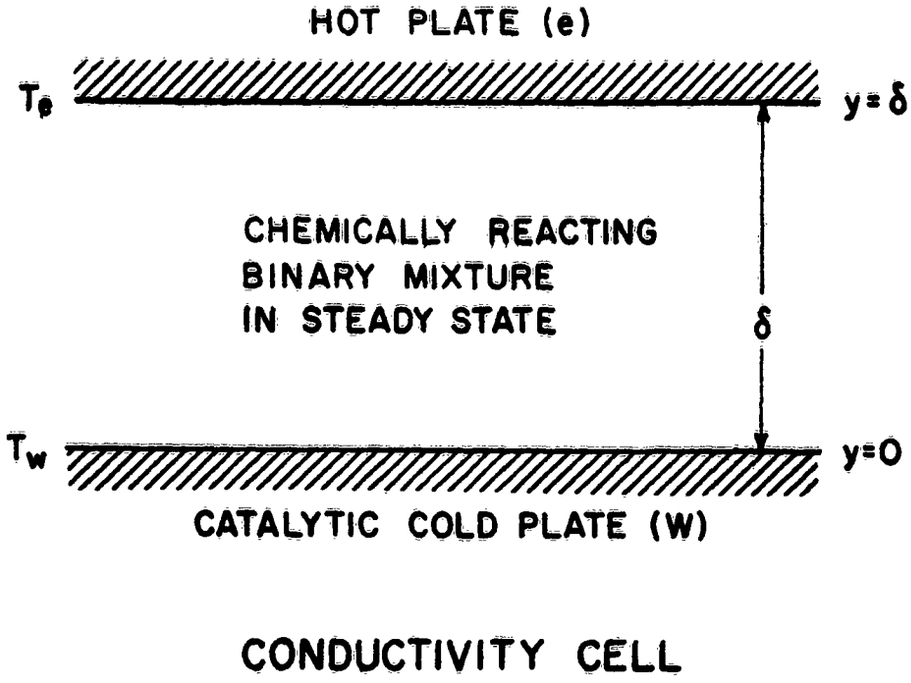

Fig. 14 Geometry and nomenclature;
thermal conductivity cell
(after Broadwell, 1958)

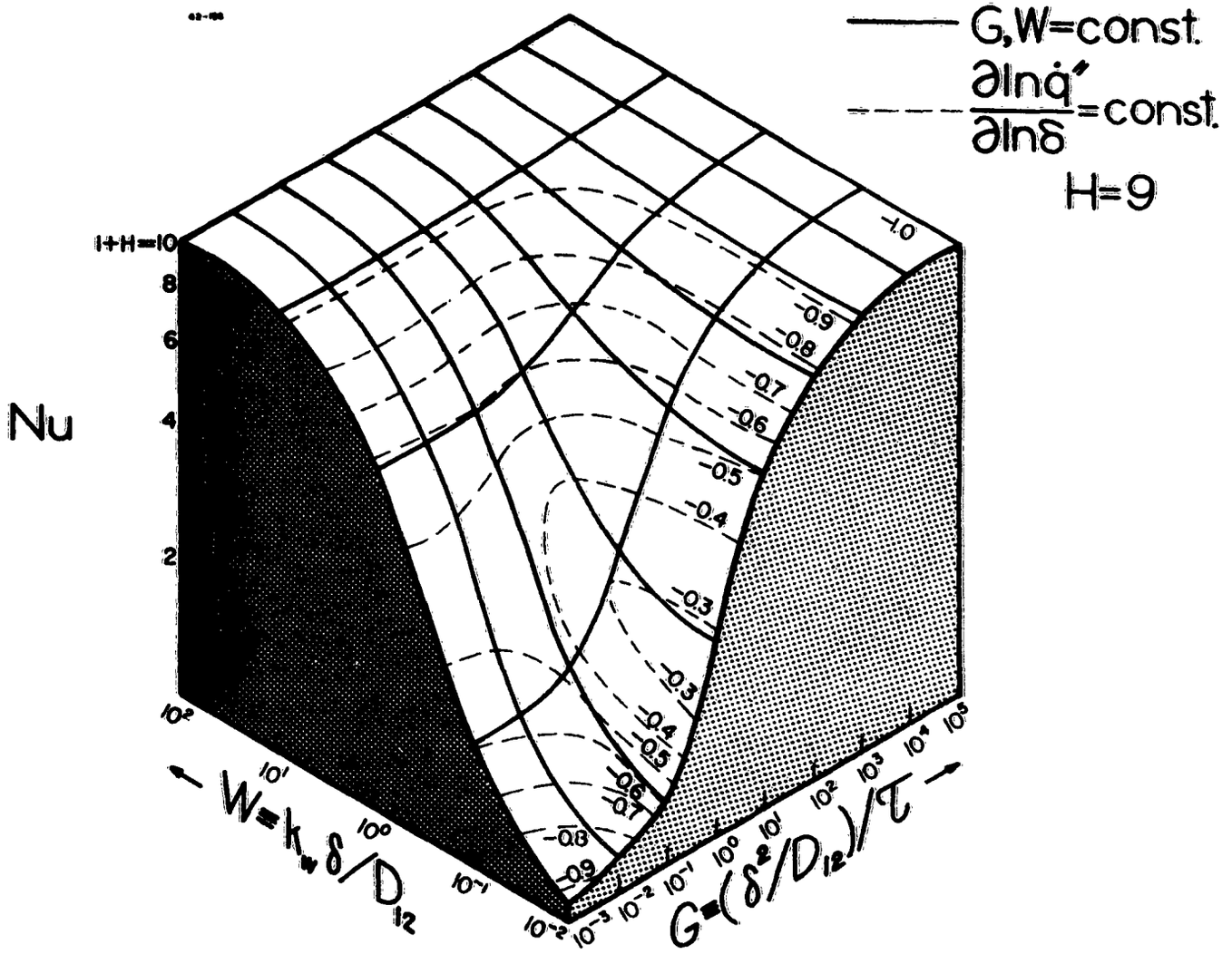

Fig. 15 Dependence of heat transfer coefficient Nu on the chemical kinetic parameters G and W; H = 9

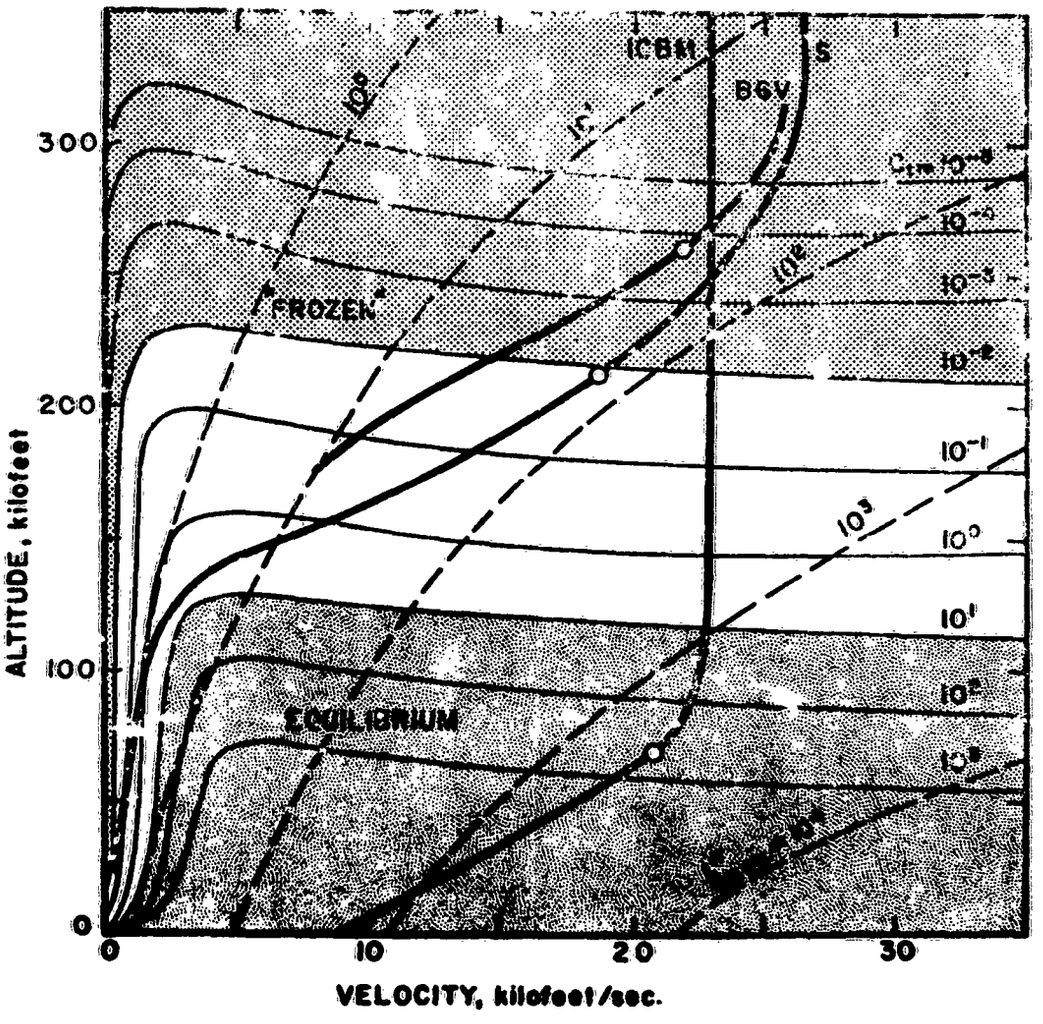

Fig. 16 Contour map of gas phase recombination parameter (24) on altitude - velocity plane (R_B = 1 ft)

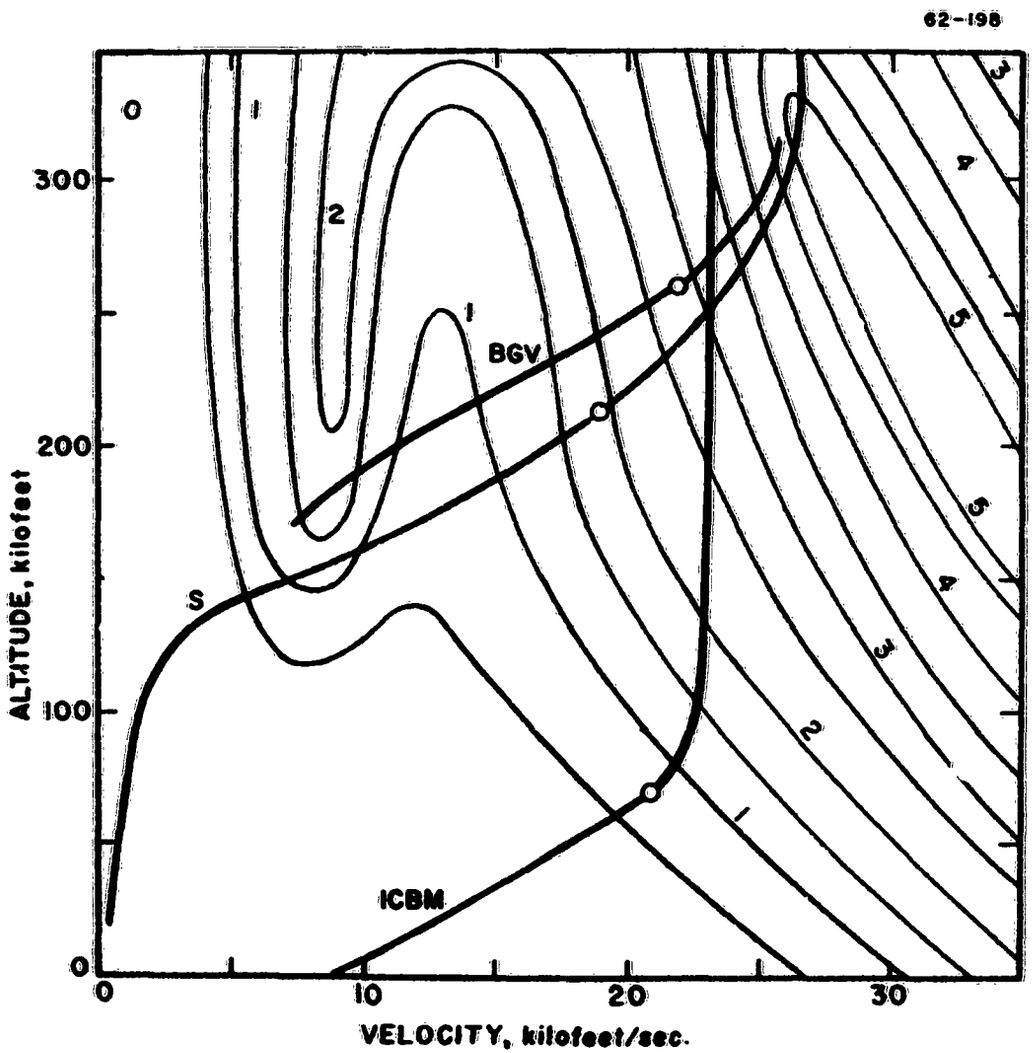

Fig. 17 Contour map of chemical enthalpy potential parameter H on the altitude - velocity plane (T_w = 1000°K)

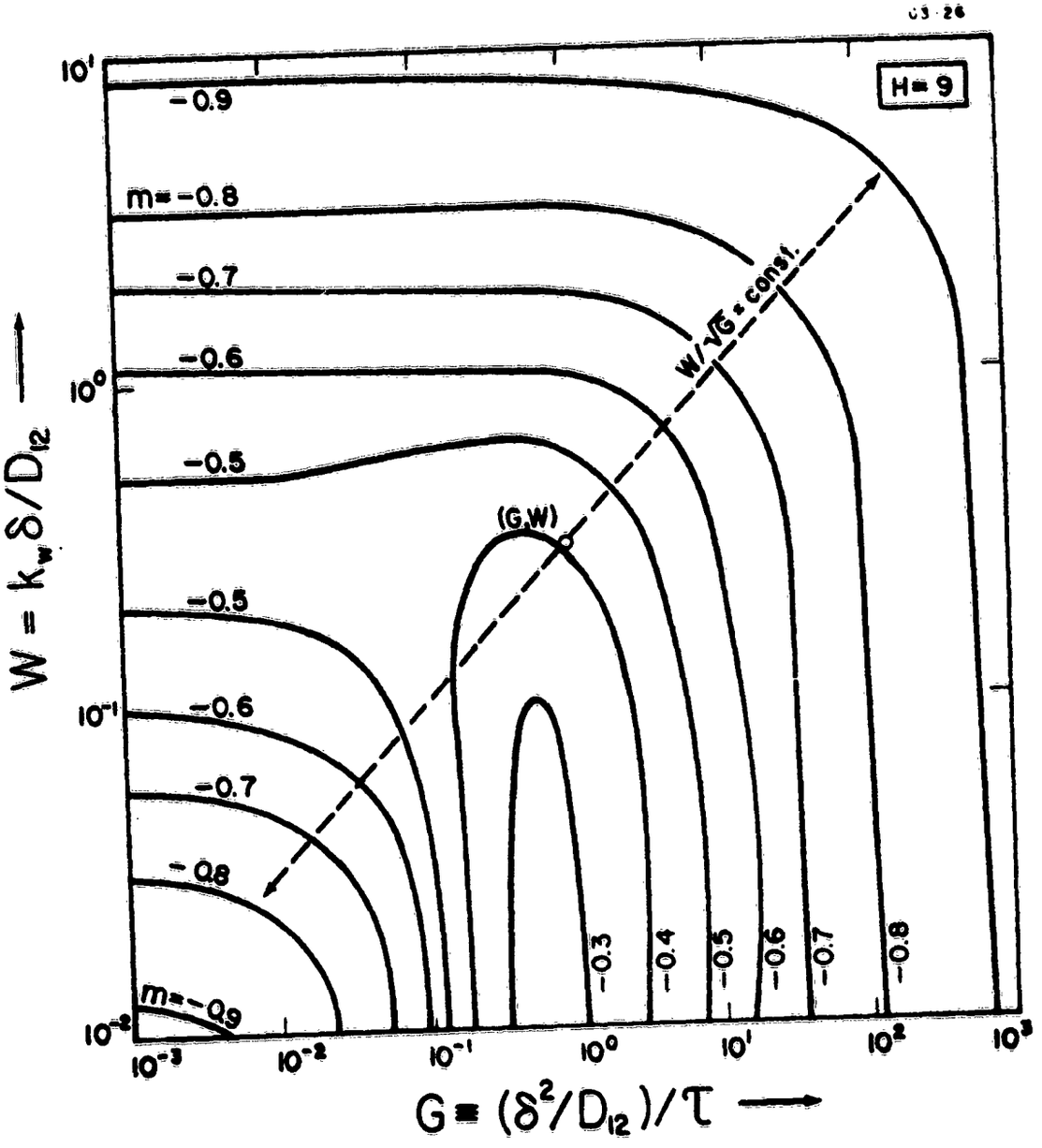

Fig. 18 Locii of constant m on the W-G plane (H = 9)

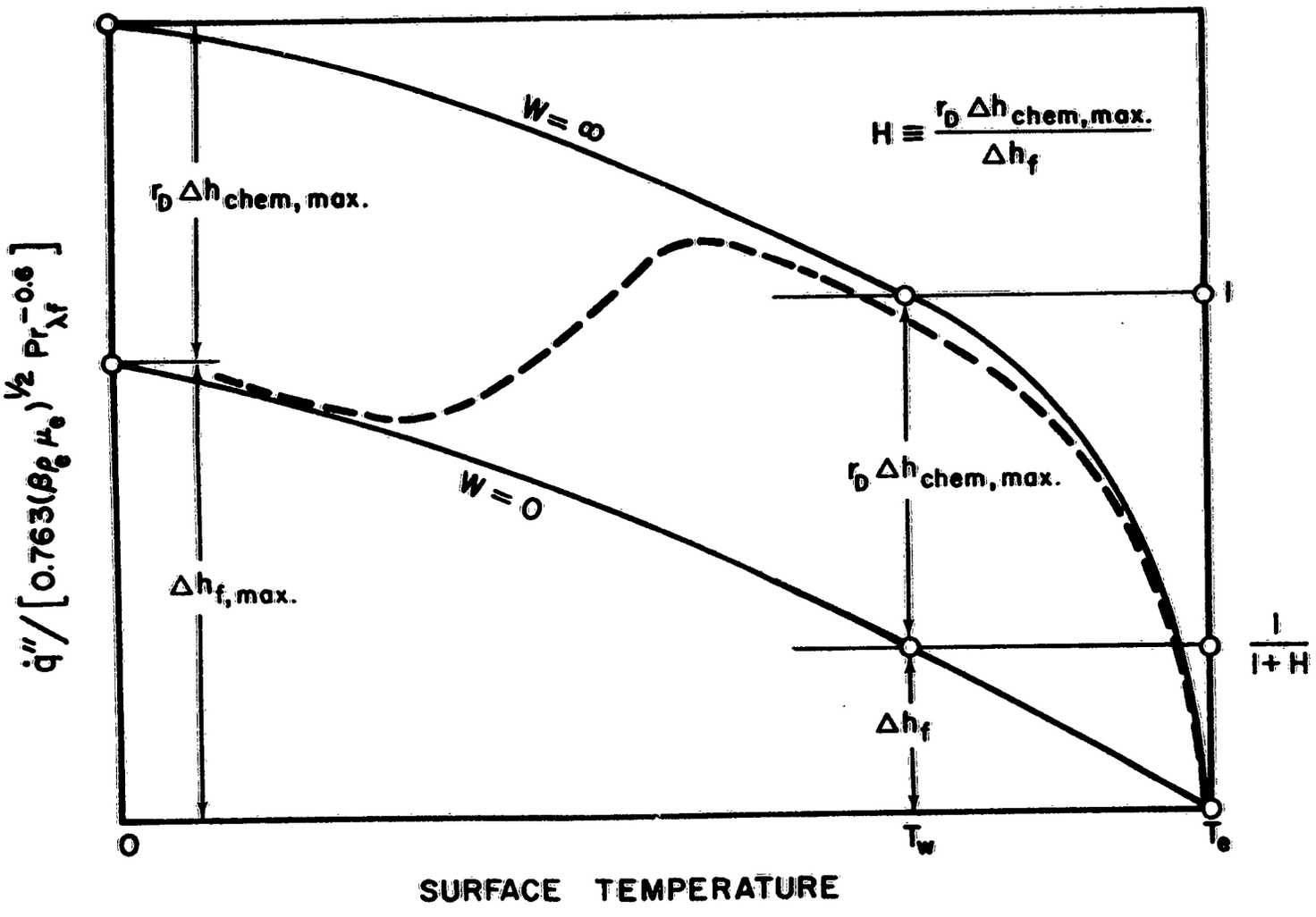

Fig. 19 Dependence of stagnation point heat flux parameter on catalyst surface temperature in the regime of chemically frozen axisymmetric, laminar boundary layer flow

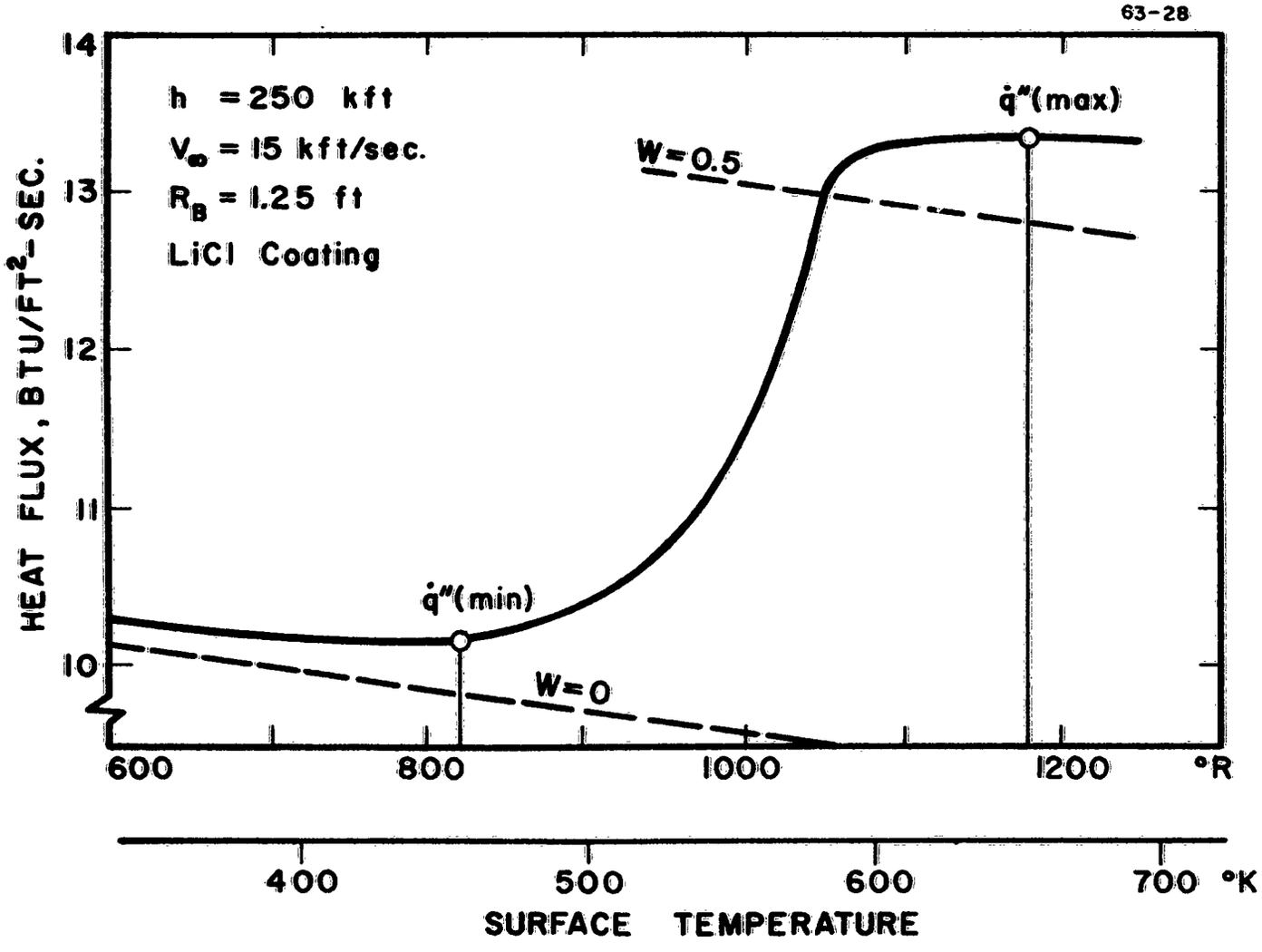

Fig. 20 Dependence of stagnation point heat flux to a LiCl surface in the regime of chemically frozen, axisymmetric laminar boundary layer flow
(R_B = 1.25 ft, h = 250 K ft; after Car son, 1962)

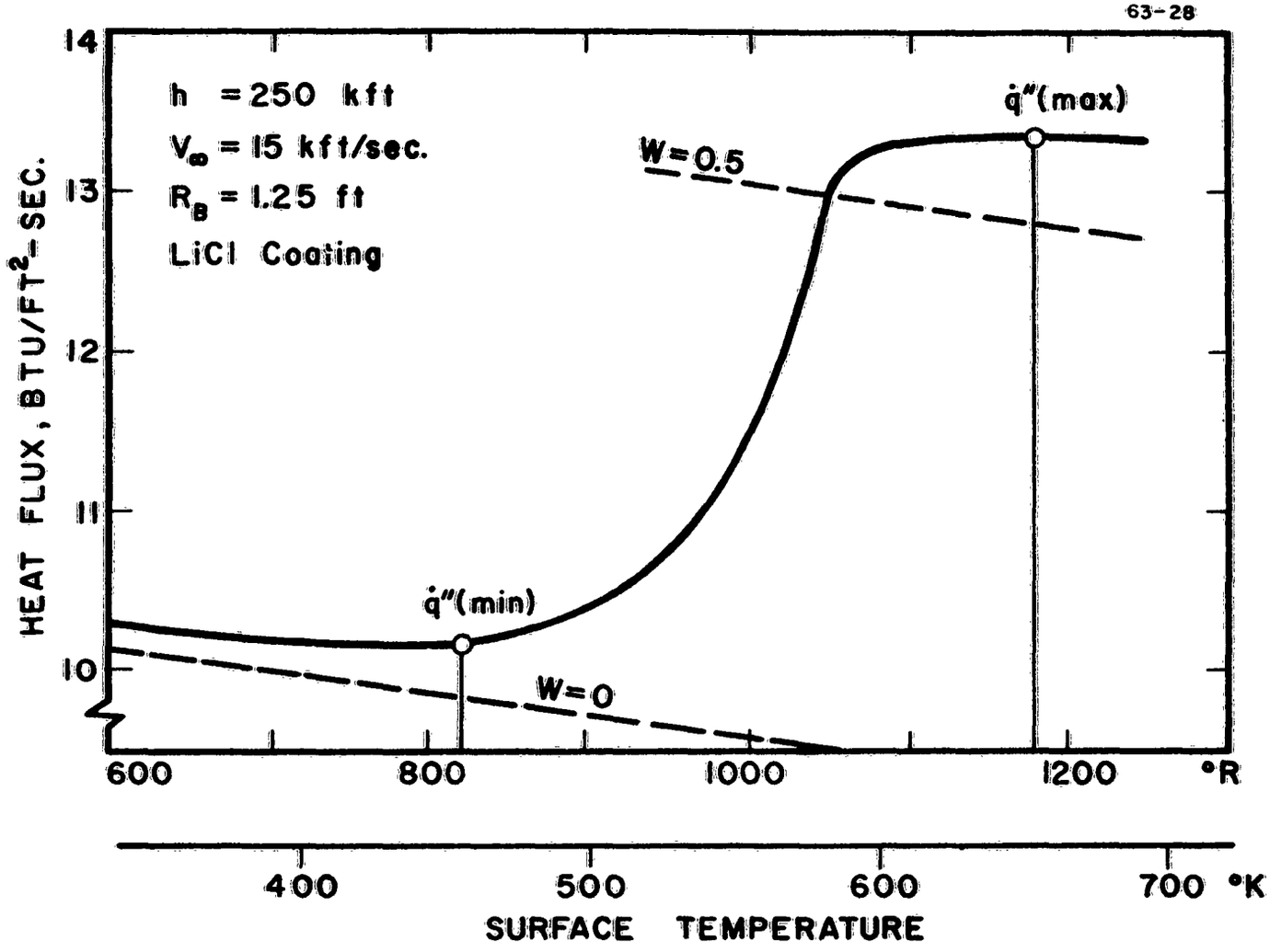

Fig. 20 Dependence of stagnation point heat flux to a LiCl surface in the regime of chemically frozen, axisymmetric laminar boundary layer flow
(R_B = 1.25 ft, h = 250 K ft; after Car son, 1962)